Novel Staufen1 ribonucleoproteins prevent formation of stress granules but favour encapsidation of HIV-1 genomic RNA

Levon G. Abrahamyan[1,2], Laurent Chatel-Chaix[1,2,3], Lara Ajamian[1,2,4], Miroslav P. Milev[1,2,4], Anne Monette[1,2,4], Jean-François Clément[1,2], Rujun Song[2,4], Martin Lehmann[1,2], Luc DesGroseillers[3], Michael Laughrea[2,4], Graciela Boccaccio[5] and Andrew J. Mouland[1,2,4,6,*]

[1]HIV-1 RNA Trafficking Laboratory, Lady Davis Institute for Medical Research-Sir Mortimer B. Davis Jewish General Hospital, Montréal, QC, H3T 1E2, Canada
[2]Lady Davis Institute for Medical Research-Sir Mortimer B. Davis Jewish General Hospital, Montréal, QC, H3T 1E2, Canada
[3]Department of Biochemistry, Université de Montréal, Montréal, QC, H3C 3J7, Canada
[4]Department of Medicine, Division of Experimental Medicine and [6]Department of Microbiology and Immunology, McGill University, Montréal, QC, H3A 2B4, Canada
[5]Instituto Leloir, IIBBA CONICET and Facultad de Ciencias Exactas y Naturales, University of Buenos Aires, Buenos Aires C1405BWE, Argentina
*Author for correspondence (andrew.mouland@mcgill.ca)

Accepted 8 November 2009
Journal of Cell Science 123, 369-383 Published by The Company of Biologists 2010
doi:10.1242/jcs.055897

Summary

Human immunodeficiency virus type 1 (HIV-1) Gag selects for and mediates genomic RNA (vRNA) encapsidation into progeny virus particles. The host protein, Staufen1 interacts directly with Gag and is found in ribonucleoprotein (RNP) complexes containing vRNA, which provides evidence that Staufen1 plays a role in vRNA selection and encapsidation. In this work, we show that Staufen1, vRNA and Gag are found in the same RNP complex. These cellular and viral factors also colocalize in cells and constitute novel Staufen1 RNPs (SHRNPs) whose assembly is strictly dependent on HIV-1 expression. SHRNPs are distinct from stress granules and processing bodies, are preferentially formed during oxidative stress and are found to be in equilibrium with translating polysomes. Moreover, SHRNPs are stable, and the association between Staufen1 and vRNA was found to be evident in these and other types of RNPs. We demonstrate that following Staufen1 depletion, apparent supraphysiologic-sized SHRNP foci are formed in the cytoplasm and in which Gag, vRNA and the residual Staufen1 accumulate. The depletion of Staufen1 resulted in reduced Gag levels and deregulated the assembly of newly synthesized virions, which were found to contain several-fold increases in vRNA, Staufen1 and other cellular proteins. This work provides new evidence that Staufen1-containing HIV-1 RNPs preferentially form over other cellular silencing foci and are involved in assembly, localization and encapsidation of vRNA.

Key words: Staufen1, HIV-1, Staufen1 HIV-1-dependent RNP, SHRNP, siRNA, Ribonucleoprotein, RNA encapsidation, Virus-host interaction, AIDS, Intracellular traffic

Introduction

The mechanisms governing the encapsidation of retroviral genomic RNAs have been the subject of intense research for many years. The principal determinants for genomic RNA (vRNA) encapsidation are an intact nucleocapsid (NC) domain in the precursor protein, $pr55^{Gag}$ (termed Gag herein) and an intact packaging signal, *psi*, within the vRNA (De Guzman et al., 1998). Recent work demonstrates that long-range interactions, conformational changes and the dimeric state of vRNA dictate the readiness for encapsidation (D'Souza and Summers, 2005; Ooms et al., 2004; Paillart et al., 2004), and the recent structure determination might help shed light on this (Watts et al., 2009). For murine leukemia virus (MLV), a network of interactions promotes sequence- and structure-specific binding by NC to the *psi* RNA. The interaction between host proteins and vRNA might also provide a molecular switch by suppressing vRNA translation to favour encapsidation (Cimarelli and Luban, 1999). There is still some controversy about whether this type of mechanism exists, because HIV-1 vRNA that is translated might also be encapsidated (Butsch and Boris-Lawrie, 2000; Kaye and Lever, 1999; Poon et al., 2002). Many questions remain concerning how HIV-1 co-opts host protein function and machineries to traffic and encapsidate its RNA genome.

Staufen1 is a double-stranded (ds)RNA-binding protein with roles in RNA localization (St Johnston et al., 1991), translation (Dugre-Brisson et al., 2005) and mRNA decay (Kim et al., 2005). It is also a principal component of RNA transport ribonucleoproteins (RNPs) (Villace et al., 2004), stress granules (SG) (Thomas et al., 2005), APOBEC3G complexes (Chiu et al., 2006) and other types of RNPs (Jonson et al., 2007; Snee and Macdonald, 2009). Staufen1 is mobile in these contexts and its presence in several types of RNPs is considered an important characteristic for performing its multiple functions (Dahm et al., 2008). Recent in vivo work also supports a role for Staufen in synapse development (Vessey et al., 2008).

In humans, there are two genes that encode Staufen1 and Staufen2 (*STAU1* and *STAU2*). Staufen2 is primarily found in neuronal cells and has roles in RNA biogenesis and trafficking (Duchaine et al., 2002; Monshausen et al., 2004). Staufen1 shares these functional characteristics but *STAU1* is more ubiquitously expressed in human tissues. Moreover, each of these genes generates a primary RNA transcript that can be differentially spliced to produce identifiable isoforms. While some work has made in-roads into deciphering the functional differences of the Staufen2 isoforms, little information is known about the functional impact of the expression of Staufen1 isoforms. Nevertheless, their existence

suggests multiple and possibly overlapping roles for these proteins in RNA biogenesis and utilization.

Evidence for a role for Staufen1 in HIV-1 replication derives from our observation that Staufen1 was incorporated in HIV-1 to levels that corresponded to the quantity of vRNA (Mouland et al., 2000). Staufen1 overexpression led to a several-fold increase in vRNA encapsidation and a corresponding decrease in HIV-1 infectivity of progeny virions (Mouland et al., 2000). In later work, we showed that Staufen1 was found in the HIV-1 RNP that contains vRNA and precursor Gag (Chatel-Chaix et al., 2004). The depletion of Staufen1 by siRNA led to defects in both virus production and infectivity (Chatel-Chaix et al., 2004). We also found that Staufen1 modulates Gag assembly (Chatel-Chaix et al., 2007), probably due to a direct interaction between the NC domain of Gag and a short region in the N-terminus of Staufen1 (Chatel-Chaix et al., 2008). The selectivity of Staufen1 to bind precursor Gag and vRNA suggested that Staufen1 performs its role in the context of a Staufen1-Gag-vRNA ternary complex and could be involved in the initial recognition and selection of vRNA during the assembly of HIV-1.

In this report, a novel Staufen1 RNP is described whose formation depends on HIV-1. Staufen1, vRNA and Gag colocalize in these Staufen1 HIV-1-dependent RNPs (SHRNPs), the size of which depends on existing Staufen1 levels in cells. A stable association between Staufen1 and vRNA was found in colocalization studies but Gag could nevertheless be displaced from SHRNPs. Staufen1 was found in various HIV-1- and stress-induced RNPs. A relationship between the abundance of virion-associated vRNA and Staufen1 and the apparent size of SHRNPs indicates that SHRNP assembly is an important event in the selection, trafficking and encapsidation of vRNA.

Results

Staufen1 depletion enhances the formation of cytoplasmic granules containing HIV-1 vRNA

Our early work in which we performed co-immunoprecipitation analyses suggested that Staufen1 interacts with HIV-1 Gag in an RNA-independent manner and forms a ternary complex with the vRNA, excluding other HIV-1 mRNA species (Chatel-Chaix et al., 2004). We developed a sequential, two-step, affinity-based immunoprecipitation assay to provide further evidence that this complex exists. We mock-transfected cells or transfected cells with HIV-1 proviral DNA with or without a Staufen1-FLAG expression construct and harvested cells for western blotting and binding analyses. We readily detected Staufen1-FLAG and Gag by western blotting and both the vRNA and *gapdh* mRNA by RT-PCR in HIV-1-expressing cells (in INPUT). Cell extracts were first submitted to an immunoprecipitation directed to the FLAG epitope. Staufen1-FLAG was first eluted from FLAG-antibody coated beads in the presence of an excess of FLAG peptide. Staufen1-FLAG was found in the first eluate (Chatel-Chaix et al., 2004), and Gag co-purified only when Staufen1-FLAG was coexpressed with HIV-1 (Fig. 1A) attesting to the specificity of Gag immunoprecipitation with the anti-FLAG resin. To examine whether the vRNA was carried through and remained associated to Staufen1-Gag, an immunoprecipitation was then performed using an anti-Gag antibody. In the final eluate, a specific RT-PCR signal for vRNA was found only when both Staufen1-FLAG and HIV-1 were coexpressed in cells, but not when Staufen1-FLAG was excluded from the transfection. This demonstrated the specificity with which vRNA co-precipitates with the anti-FLAG and anti-Gag antibodies. The result provides corollary biochemical evidence that a Staufen1-Gag-vRNA ternary complex exists in HIV-1-producing cells. To confirm the existence of this ternary complex and to better characterize it, we examined the localization of Staufen1 in relationship to vRNA and Gag in situ by using combined immunofluorescence and fluorescence in situ hybridization analyses (IF/FISH) followed by laser scanning confocal microscopy (LSCM). In control (siNS-treated) HIV-1-expressing cells, Staufen1, Gag and vRNA exhibited colocalization in the cytoplasm and prominent colocalization at the plasma membrane. Imaging analyses demonstrated that these viral and host components are found as a ternary complex in HIV-1-producing cells (Fig. 1B). These observations extend our earlier work that showed that Staufen1 associates selectively with these viral components in cells (Chatel-Chaix et al., 2004; Mouland et al., 2000). Whereas the diameter of Staufen1-positive punctae in mock-treated (non-HIV-1-expressing) cells was determined to be less than 200 nm, in HIV-1-expressing cells Staufen1, Gag and vRNA were generally found in small punctae of approximately 0.6-0.7 μm (Fig. 1B,E).

We next examined the effects on HIV-1 vRNA and Gag localization of depleting cells of both Staufen1 isoforms by using si55/63, or of the high molecular weight Staufen1^{63kDa} alone by using si63. HeLa cells were mock-transfected or transfected with proviral DNA and non-silencing control siRNA (siNS), si55/63 or si63. Staufen1 depletions were always verified by RT-PCR and/or western blotting (Fig. 1C). RT-PCR analyses showed that the siRNAs specifically targeted *Staufen1* mRNAs as expected, with si55/63 targeting the expression of *Staufen1*^{55kDa} and *Staufen1*^{63kDa} transcripts and si63 targeting uniquely the *Staufen1*^{63kDa} (T3) transcript. The depletions of Staufen1 by si55/63 or si63 were consistent, selective and highly efficient (depletions of 90-92%).

In our imaging analyses, we found an apparent doubling in the size of granules for the RNPs that were enriched in vRNA, Gag and the residual Staufen1 in si55/63-treated cells and these were principally found in juxtanuclear and cytoplasmic domains (Fig. 1D,E). Strikingly, in 90±5% (mean ± s.e.m., n>250 cells) of the cells, we only found Staufen1-containing RNPs in HIV-1-expressing cells (white arrowheads, Fig. 1D) and not in cells in which HIV-1 expression was not detectable (yellow arrowheads, Fig. 1D, si55/63 panels). Residual levels of Staufen1 and Gag appeared in large bright punctae due to accumulations of these proteins in these foci. We also examined SHRNPs in Jurkat T cells, and found that these were enlarged when Staufen1 was depleted by short hairpin (sh)RNA (shSTF; data not shown); however, the paucity of cytoplasmic space limited our conclusions from the results obtained using this cell type. The localization of Staufen1, vRNA and Gag in Staufen1^{63kDa}-depleted HeLa cells did not markedly change SHRNP appearance in greater than 90% of cells examined (>200 cells, five experiments; Fig. 1D, bottom panel). Identical findings for Staufen1 depletions and SHRNP formation were obtained at 24 and 48 hours post-transfection (Fig. 1E). These results demonstrate that larger intracellular RNPs form that contain vRNA and the residual Staufen1, primarily when both Staufen1 isoforms are silenced in cells. We cannot completely rule out the possibility that the strong signal intensities were due to coalescing RNPs or other organelles at these foci. Because Staufen1, vRNA and Gag colocalize in cytoplasmic punctae and at the periphery in HIV-1-producing cells, we therefore named these RNPs Staufen1 HIV-1-dependent RNPs (SHRNPs).

Results from our Manders' colocalization analyses were also consistent, such that while Staufen1 and vRNA colocalized

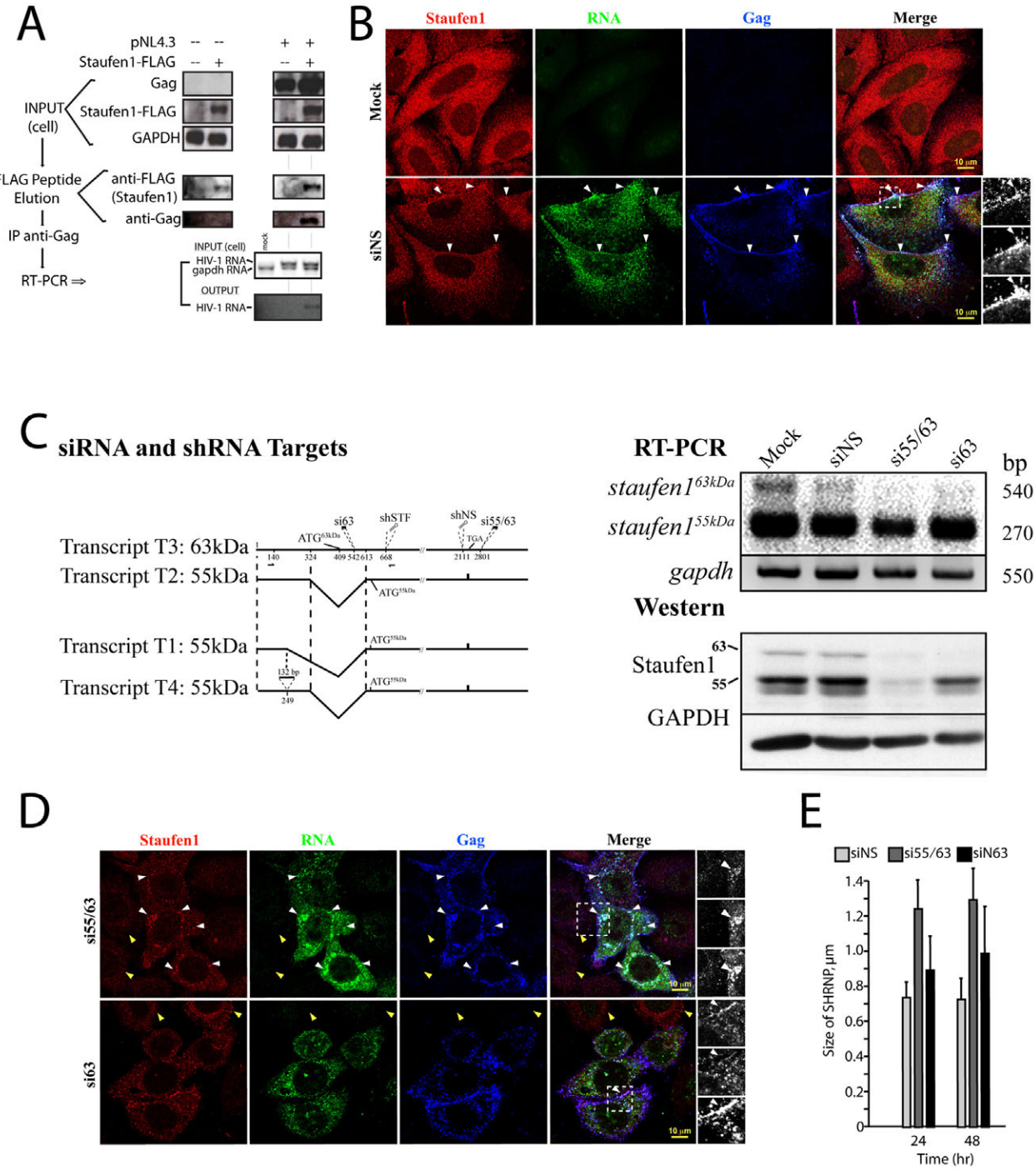

Fig. 1. Staufen1, vRNA and Gag are part of the same ternary complex and colocalize in cells. (**A**) HeLa cells were mock-transfected or transfected with pNL4-3 proviral DNA without (–) or with (+) Staufen1-FLAG. A sequential Staufen1 and Gag binding assay was performed as described in Materials and Methods. Gag, Staufen1-FLAG and GAPDH were quantified by western blotting in Input lanes and Staufen1-FLAG and Gag were identified following FLAG elution and Gag immunoprecipitation (IP). vRNA and *gapdh* RNAs (loading control) were detected by RT-PCR in cellular extracts before analysis and in the final eluted IP complexes. (**B**), HeLa cells were mock-transfected or co-transfected with the HxBRU proviral DNA and siNS, si55/63 or si63. Cells were harvested and fixed. Staufen1 (red), vRNA (green) and Gag (pseudocoloured blue) were imaged by LSCM at 48 hours in mock- and siNS-treated cells. White arrowheads identify regions of colocalization (magnifications are shown in insets). (**C**) Four Staufen1 transcripts are shown (T1-T4). The T3 variant encodes Staufen1^{63kDa} due to an upstream ATG initiation codon (position 409). The other transcripts encode Staufen1^{55kDa}. siRNAs (si55/63, si63) or shRNAs (shNS, shSTF) are depicted above the T3 transcript. The positions of forward and reverse primers used for semi-quantitative RT-PCR analyses to quantify *Staufen1* mRNAs are shown below T3. On the right is shown RT-PCR and western analyses of *Staufen1*^{63kDa} and *Staufen1*^{55kDa} mRNAs and gene products in mock- and siRNA-treated cells. *gapdh* mRNA and GAPDH are loading controls. PCR yields a 540 bp product for T3 or a 270 bp PCR product for the shorter *Staufen1* mRNAs. (**D**) Staufen1 (red), vRNA (green) and Gag (blue) were imaged at 48 hours in si55/63- and si63-treated cells. Large SHRNP foci are indicated by white arrowheads in si55/63-treated and/or HIV-1-expressing cells. HIV-1-negative cells are indicated by yellow arrowheads. Insets represent high-resolution black and white depictions of cell regions (dashed boxes). (**E**) Histograms show the average size of Staufen1 granules. The error bars represent s.d. Scale bars: 10 µm.

appreciably to 20±9.1% (mean ± s.e.m.) in siNS-treated cells, there was a tripling to 58% of the proportion of Staufen1 colocalizing with vRNA in conditions of si55/63 depletion (Table 1). This increase also shows that there was little redistribution or loss of Staufen1 from the vRNA-Gag complex in depletion conditions.

SHRNPs are in equilibrium with polysomes and are distinct from stress granules

Viral infection can generate a cellular stress response (Gale et al., 2000; McInerney et al., 2005) and Staufen1 is a component of SGs (Thomas et al., 2005). Recent data show that Staufen1 might temper stress responses in cells by controlling the equilibrium between the formation of polysomes and SGs (Thomas et al., 2009). To determine whether SHRNP assembly in Staufen1-depleted cells depends on translation activity, a characteristic of SG assembly, HeLa cells were transfected with HIV-1 proviral DNA and siRNAs as above and left untreated, or briefly treated with puromycin (Pur) or cycloheximide (CHX) to promote or inhibit SG assembly, respectively. IF/FISH co-analyses were performed to identify Staufen1, Gag or PABP1 (a marker for SG) and vRNA. On the one hand, Pur treatment induced PABP1- and Staufen1-containing SG and these were observed when HIV-1 was expressed and in Staufen1-depleted cells (Fig. 2, panels 2-4). On the other hand, a translation block at the level of elongation induced by CHX treatment caused a uniform distribution of PABP1 as expected. The distribution of Staufen1 was likewise dispersed in this condition when HIV-1 was expressed (Fig. 2, panels 5-7). These data indicate that SHRNP assembly is dependent on translation and appears to be in equilibrium, like SG, with cellular mRNA translational activity.

To determine whether vRNA was included in the Staufen1-PABP1-containing foci, we next examined its localization under these experimental conditions. Without drug treatment, HIV-1 expression did not elicit a stress response in cells because large PABP1+ or Staufen1+ SG foci were not detectable (data not shown and Fig. 3A, panel 2). In untreated cells, we observed identical distributions for Staufen1, Gag and vRNA as shown in Fig. 1D for siNS, si55/63 and si63 conditions, respectively (Fig. 3A, panels 2-4). Pur treatment resulted in the formation of 2- to 5-μm structures containing Staufen1 in mock-transfected cells (Fig. 3A, panel 5) and caused a near-complete recruitment of vRNA and Staufen1 to Pur-induced SGs (Fig. 3A, panels 6-8) containing PABP1 (because PABP1 is also colocalized with Staufen1; see Fig. 2, panels 2-4) in HIV-1-expressing cells. Strikingly, Gag was almost completely excluded from SGs in Pur-treated HIV-1-expressing cells, demonstrating that the Staufen1-vRNA association is maintained under Pur treatment. In Staufen1-depleted and Pur-treated cells, the residual Staufen1 was also recruited to PABP1-positive SG foci together with vRNA (Fig. 2, panel 4; Fig. 3A, panel 7). This suggested that the prominent SHRNPs in Staufen1-depleted cells (no drug added) can be remodelled and that Staufen1 and vRNA can be recruited from Gag-containing SHRNPs to constitute SGs. This is consistent with the ability of Staufen to shuttle from RNA trafficking granules to SGs in response to stress (Thomas et al., 2005). Thus, the Pur-induced SGs containing Staufen1, vRNA and PABP1 are probably bona fide SGs, and the association between Staufen1 and vRNA remains stable in the context of both SHRNPs and Pur-induced SGs. In the latter, however, Gag is not present, and this was reflected by our sequential affinity-immunoprecipitation assay (data not shown and Fig. 1A). Consistently, we did not find a significant change in the colocalization between Staufen1 and vRNA in untreated and Pur-treated cells (Table 1). These results indicate that the Staufen1-containing RNPs undergo remodelling and that the composition of a SHRNP is distinct from that of a Pur-induced SG.

When cells were treated with CHX to block translation elongation, highly dispersed distributions for PABP1 (Fig. 2), vRNA and Gag were found. Few SG formed in all conditions and the SHRNPs in Staufen1-depleted cells were less numerous (Fig. 3, panels 9-12). The brief treatments with Pur or CHX had little impact on steady-state levels of Gag protein (Fig. 3B). These results further demonstrate a dependence on translation for SHRNP formation.

Table 1. Staufen1 and vRNA colocalization* analyses

Treatment	Staufen1 with vRNA (% ± s.d.)	vRNA with Staufen1 (% ± s.d.)
Provirus pNL4-3		
siNS	20±9.1	65±13.1
si55/63	58±15.7	66±15.1
siNS + Pur	24±7.1	44±7.1
si55/63 + Pur	23±9.1	45±8.1
HIV-1 + Ars	28±13.1	62±8.1
Provirus pNL4-XX (Gag^{-}, Gag/Pol^{-})		
siNS	26±7	nd
si55/63	60±10	nd

*Manders' colocalization coefficients were calculated as described in Materials and Methods.
Ars, arsenic; Pur, puromycin; nd, not determined.

HIV-1 prevents formation of SGs and processing bodies

The exposure of cells to arsenic (Ars) is known to induce the formation of SGs that contain Staufen1, PABP1 and other proteins such as HuR, G3BP and eIF3 (Anderson and Kedersha, 2008; Kedersha et al., 2002; Thomas et al., 2005). Because SHRNPs and SGs are related by virtue of the presence of Staufen1 in these cytoplasmic foci, we determined what the outcome was on Staufen1, Gag and vRNA localization by treating HIV-1-producing cells with Ars. In mock-transfected cells we first confirmed that Ars treatment induced visible SGs enriched in both Staufen1 and PABP1 (Fig. 4A). Strikingly, however, in cells expressing HIV-1 (i.e. staining for vRNA and Gag; Gag staining is not shown), we were not able to find typical Ars-induced SGs in either siNS or si55/63 conditions. Here, vRNA and Staufen1 were dispersed and accumulated at a juxtanuclear region in cells in about 95% of cells (Fig. 4B,C; white arrowheads; n=150-200). Thus, HIV-1 expression prevents the formation of SG foci that are induced by Ars. The extent to which Staufen1 and vRNA colocalized was not different to that found in untreated cells (Table 1), indicating that a redistribution of these SHRNPs had occurred. In 85% of transfected cells (n=200), large Staufen1 (and PABP1-positive, not shown) SGs were detectable in HIV-1-negative cells (e.g. yellow arrowheads in Fig. 4B-D), similar to those found in mock-treated cells (Fig. 4A, right panel). In addition, a deficit in Staufen1 did not impede SG formation per se, consistent with recent findings (Thomas et al., 2009), nor did it change the abundance of SGs. However, HIV-1 changed the characteristics and location of Staufen1-containing RNPs. These data also demonstrate that HIV-1-expressing cells are resistant to Ars-induced SG formation. Finally, PABP1 staining in these vRNA and Staufen1 RNPs was virtually absent compared with that in the surrounding cytoplasm, indicating that these RNPs did not bear this hallmark SG marker (Fig. 4E). This was in contrast to the inclusion

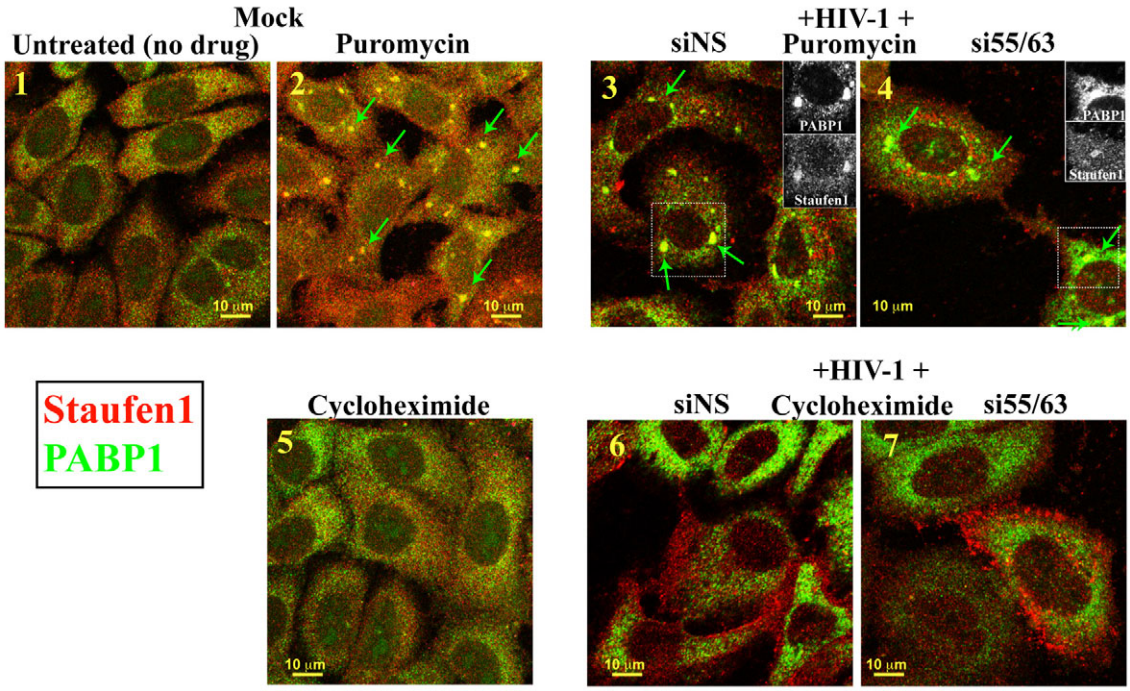

Fig. 2. SHRNPs are not SG. HeLa cells were mock-transfected (panels 1,2) or transfected with HxBRU DNA and siNS (panel 3) or si55/63 (panel 4). Cells presented in panels 2-4 were incubated with Pur before fixation. Insets show black and white renditions for PABP1 and Staufen1 staining in boxed areas. Cells shown in panels 5-7 were treated with CHX before fixation. Cells were fixed and stained for Staufen1 (red), PABP1 (green) and Gag (not shown). Large yellow granules in panels 2-4 represent colocalized Staufen1-PABP1 foci induced by Pur treatment. Arrows identify SG induced by Pur. Scale bars: 10 µm.

of PABP1 (and the exclusion of Gag) in Pur-induced SGs (Fig. 3). The block to the formation of Ars-induced SGs by HIV-1 was confirmed using other SG proteins such as eIF3 and G3BP (Anderson and Kedersha, 2008) (supplementary material Fig. S1). Moreover, the HIV-1-induced block to SG formation supports the notion that SHRNPs are distinct in HIV-1 producing cells because they also exclude four SG marker proteins tested in this work (PABP1, G3BP, eIF3 and HuR) (Fig. 4 and supplementary material Fig. S2).

It is known that SG formation and translational inhibition after Ars treatment is dependent on eIF2α phosphorylation, the reduction of the translation ternary complex, and recruitment of several RNA-binding proteins (Kedersha et al., 1999). Some viruses have developed mechanisms to replicate during cellular stress even when cellular translation is shut off by eIF2α phosphorylation (McInerney et al., 2005). We analyzed the levels of phosphorylated eIF2α (eIF2α-*P*) in cells. This analysis revealed that Ars treatment induced eIF2α-*P* almost threefold (293%). Although HIV-1 alone did not induce eIF2α-*P* levels to any great extent (121%), HIV-1 did not markedly alter eIF2α-*P* levels in Ars-treated cells either (230% vs 293%), demonstrating that HIV-1 expression does not protect cells from SG formation by inhibiting eIF2α phosphorylation (Fig. 4F).

The processing body (PB) represents another type of RNP complex that plays a role in RNA storage and metabolism. PBs have been posited to be important for replication of Ty retrotransposons and for other RNA viruses (Beckham and Parker, 2008; Beliakova-Bethell et al., 2006). Staufen1 has also been found in *Drosophila* PBs but not in those in mammalian cells (Barbee et al., 2006; Thomas et al., 2009). We therefore attempted to clarify whether the Staufen1-containing SHRNPs were related to PBs by staining cells with a classical PB marker, DCP-1. HeLa cells were transfected with HIV-1 DNA and siRNAs as described above, and PBs were detected using an anti-DCP-1 antibody by indirect IF and LSCM. As shown in Fig. 5A, there was no significant colocalization between vRNA, Gag or Staufen1 and DCP-1 in either control or Staufen1-depleted cells (Fig. 5A). We then counted the number of PBs in cells in which we detected DCP-1 foci. In mock-transfected cells, the average number of PB foci in a single LSCM focal plane through the middle of the cell (as judged by confocal sectioning along the Z-axis) totalled 28±1 (mean ± s.e.m.) foci per cell. By contrast, the number of PBs dramatically reduced to 7±1 (mean ± s.e.m.), when we counted all cells expressing DCP-1 at low and high levels in HIV-1-expressing cells. In other imaging experiments, we observed few – if any – PBs in HIV-1-expressing cells labelled with vRNA (Fig. 5B). Likewise, the effects of HIV-1 on PB abundance are probably due to effects on PB assembly because the abundance of DCP-1 in cells was maintained (in both transfected HeLa and infected Jurkat T cells; Fig. 5B and data not shown).

Ars treatment of cells dramatically induces the number of visible PB foci in cells. In addition, it promotes the formation of Staufen1- and PABP1-positive SGs. The relationship between SHRNPs and PBs was therefore analyzed after stress induction by Ars. We could not find PBs at the juxtanuclear region in Ars-treated cells, which was where vRNA, Gag and Staufen1 were found (Fig. 5C, panels 1,2). In mock-transfected cells, PABP1 staining was dispersed and PBs were detectable (Fig. 5B, panels 3,4), whereas in mock-transfected cell treated with Ars, we observed PBs in close proximity to numerous PABP1-positive SGs (Fig. 5C, panels 5,6, indicated by yellow arrowheads), confirming that SGs and PBs are dynamically linked (Kedersha et al., 2005). Our results

demonstrate that in HeLa cells, vRNA and Gag do not localize to PBs, and SHRNPs do not contain DCP-1 and therefore are probably not PBs. Cumulatively, our results suggest that HIV-1 impairs the formation of constitutive or stress-induced silencing foci. By regulating the equilibrium between SGs, PBs and other RNPs, HIV-1 could efficiently exploit the cellular machinery to ensure efficient virus assembly when cells are exposed to different types of stresses.

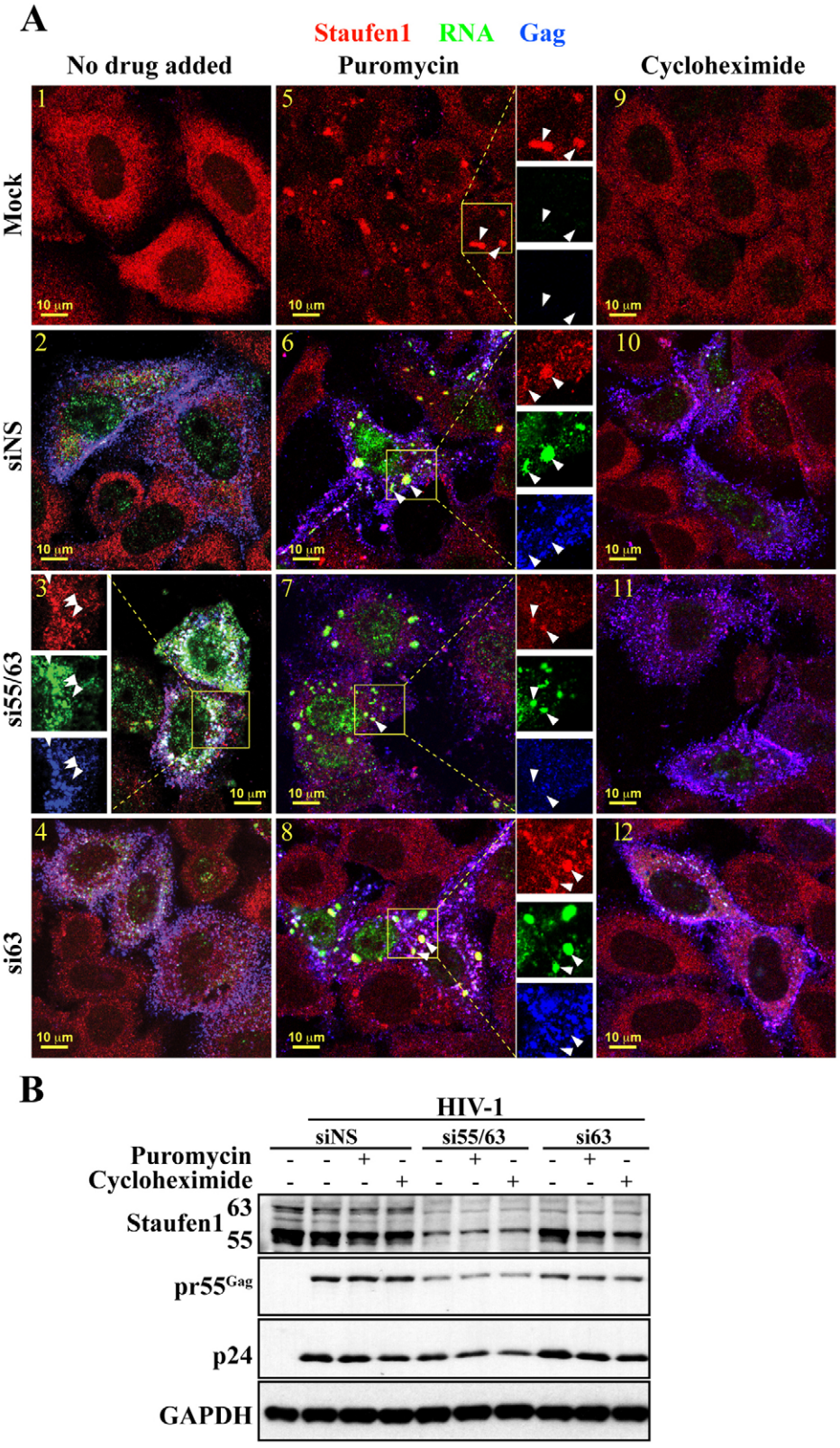

Fig. 3. Pur induces the formation of large granules containing Staufen1 and vRNA but not Gag. HeLa cells were transfected as in Fig. 1. (**A**) Combined IF/FISH co-analyses for Staufen1 (red), Gag (blue) and vRNA (green) in untreated cells (panels 1-4) or cells treated with Pur (panels 5-8) or CHX (panels 9-12). Staufen1, Gag and vRNA accumulated in large granules in si55/63 conditions (white arrowheads in panel 3 and corresponding insets). In Pur-treated cells, Staufen1 was found in SG (red granules in panel 5 indicated by yellow arrowheads). The yellow granules in panels 6-8 correspond to Staufen1 and vRNA colocalization in SG induced by Pur treatment, but Gag was excluded from these SG (white arrowheads in panels 6-8 and corresponding insets). Insets are 1.5× magnifications. (**B**) Corresponding protein expression levels for Staufen1, Gag and GAPDH (loading control). Scale bars: 10 μm.

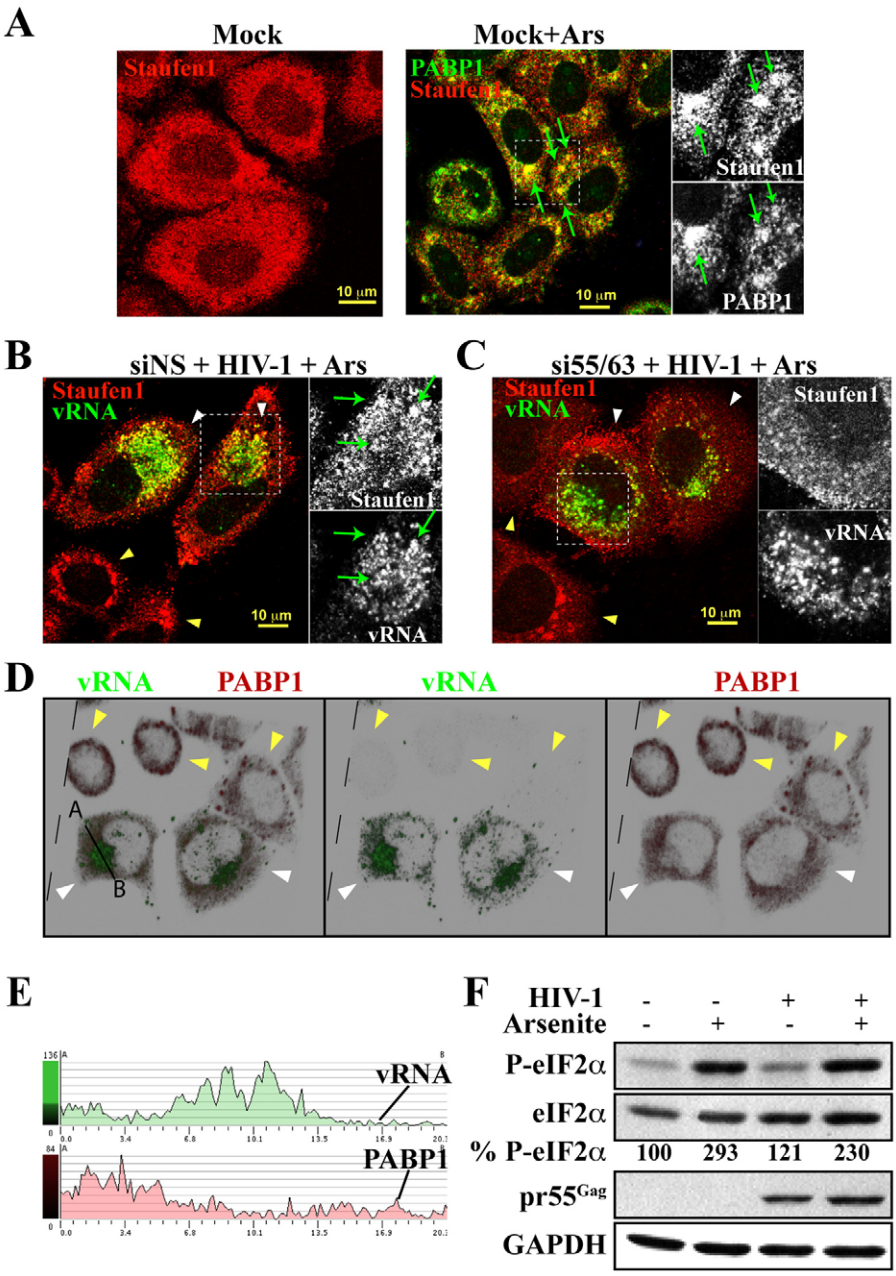

Fig. 4. HIV-1 prevents SG formation. (**A**) HeLa cells were transfected as in Fig. 1. Cells were incubated with Ars and then allowed to recover before fixation. (**A**) Staining for Staufen1 in mock-treated cells (left panel) or for Staufen1 and PABP1 in cells treated with Ars (right panel). Arrows identify typical SG enriched in Staufen1 and PABP1. Insets show black and white renditions of Staufen1 and PABP1 foci. (**B**,**C**) Staufen1 and vRNA localization in Ars-treated, HIV-1-expresing cells transfected with siNS or si55/63. Insets show staining of Staufen1 and vRNA. White arrowheads indicate accumulations Staufen1 and vRNA RNPs in the juxtanuclear region in HIV-1-expressing cells. (**D**) Normal shading was applied to original confocal images of cells generated using Imaris software for Ars-treated, HIV-1 expressing cells showing PABP1 staining (red) and vRNA staining (green). HIV-1-expressing cells are indicated by white arrowheads. Yellow arrowheads identify Ars-induced SG in non-producing cells. Dashed lines demarcate image limit. (**E**) Intensity plots for PABP1 and vRNA staining from point A to B (shown in D) in cell are shown. (**F**) Corresponding western blot analyses for eIF2α-*P* (P-eIF2α), eIF2α, Gag and GAPDH are shown. Numbers below the eIF2α bands indicate relative levels of eIF2α-*P* and are derived from the ratio of eIF2α-*P* to eIF2α signal intensities ×100%. eIF2α-*P* levels found in untreated, mock-transfected cells were set to 100%. GAPDH is loading control. Scale bars: 10 μm.

Gag expression is decreased after Staufen1 depletion

The depletion of both Staufen1 isoforms by si55/63 resulted in markedly diminished Gag expression levels (53±5%, mean ± s.e.m., five experiments; Fig. 6). Staufen1^{63kDa} depletion alone had little effect on Gag expression (84±2.5%, mean ± s.e.m., five experiments) and both treatments had little effect on gp120 (Env) expression levels in the context of pNL4-3 (Fig. 7 and data not shown). The effects on Gag expression cannot be explained by the activation of the Jak-Stat pathway and the expression of IFN-inducible genes like PKR, by changes in the cell cycle or by changes in Gag protein stability (data not shown). Because we have shown that Staufen1 can enhance translation of certain mRNAs (Dugre-Brisson et al., 2005) and can stabilize polysomes (Thomas et al., 2009), these changes are probably due to effects of Staufen1 depletion on HIV-1 vRNA translation.

Staufen1 and vRNA assemble without Gag

Gag has a central role in assembly and virus structure and this is substantiated by its ability to bind and co-opt many cellular proteins, including Staufen1 (Chatel-Chaix et al., 2004). Our observation that Gag could be rapidly excluded from Staufen1-vRNA RNPs by a brief Pur treatment revealed that these RNPs are dynamic and plastic structures. We therefore determined whether Staufen1-vRNA RNPs could form in the absence of Gag expression and also questioned whether PABP1 could replace Gag when it is not expressed. In order to do this, we expressed a pNL4-3-based proviral DNA (pNL4-XX) in which Gag expression is prevented due to the introduction of two stop codons in the *gag* open reading frame. This vector expresses all HIV-1 RNAs, and aborted translation of the vRNA prevents the synthesis of Gag and Gag-Pol proteins but the translation of 4 and 2kb RNAs is not impaired

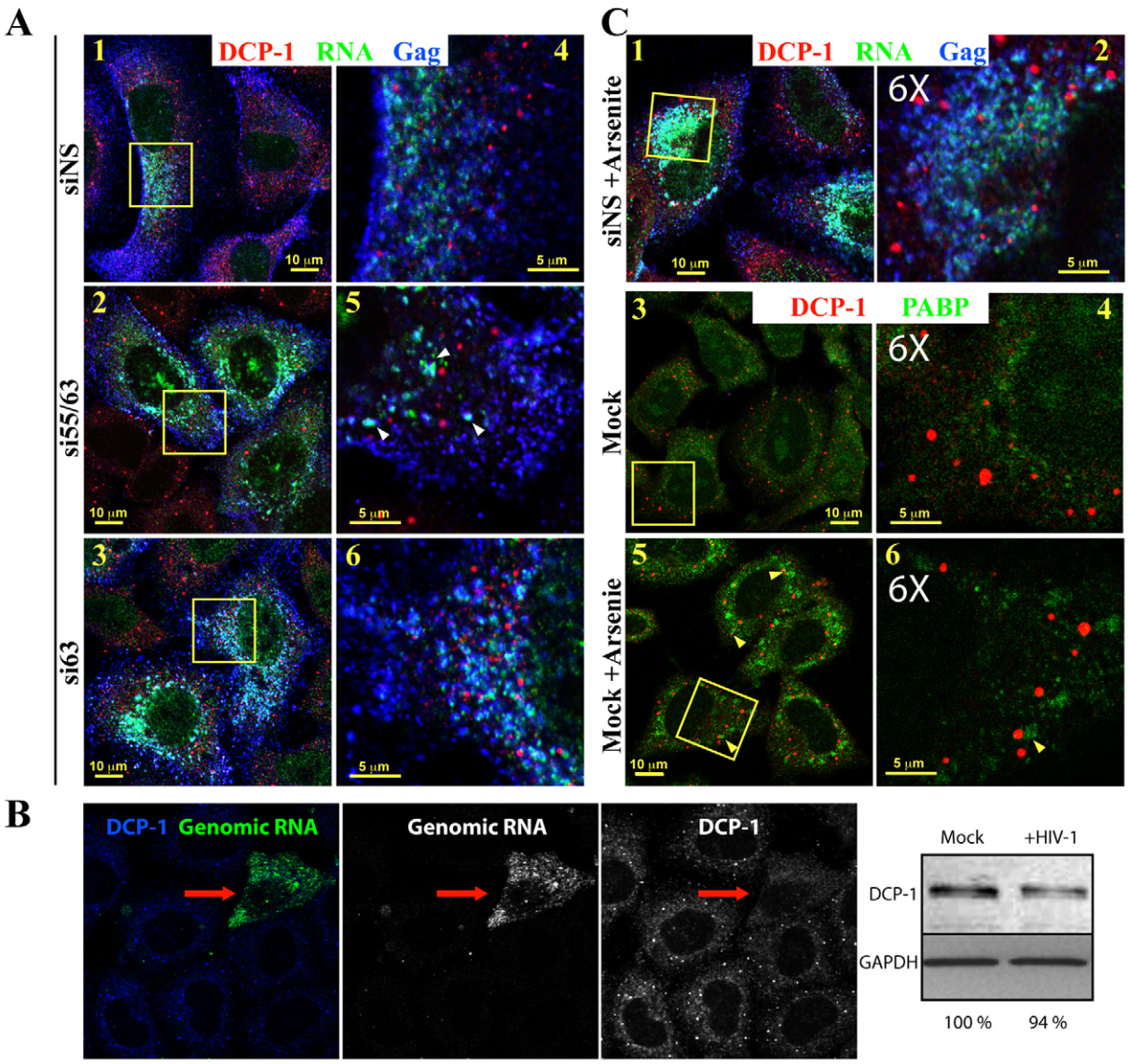

Fig. 5. SHRNPs are distinct from PBs, and Gag and vRNA are not localized to PBs. (**A**) Staining for PB in HIV-1-expressing cells transfected with siNS, si55/63 or si63. Panels 4-6 show 6× magnifications of boxed areas. White arrowheads indicate large granules containing vRNA and Gag in Staufen1-depleted cells. (**B**) Left: DCP-1 (red) was localized in a HIV-1-expressing cell (vRNA in green). Right: DCP-1 expression levels were evaluated by western blotting with GAPDH as a loading control. Percentages indicate relative levels of DCP-1. (**C**) Panels 1 and 2: Staining for DCP-1 (red), vRNA (green) and Gag (blue) in HIV-1-expressing (siNS) and Ars-treated cells. vRNA, Gag and DCP-1 staining in the juxtanuclear region is shown in Ars-treated cells with DCP-1 staining (panel 1; 6× magnification of boxed region in panel 2). Panels 3-6 show DCP-1 and PABP1 staining in mock-transfected cells without or with Ars-treatment. SG are indicated by yellow arrowheads (compare panels 3,4 with panels 5,6). Scale bars: 10 µm (A1-3, C1,3,5); 5 µm (A4-6, C2,4,5,6).

(Ajamian et al., 2008). Following expression of pNL4-XX in siNS and si55/63 conditions, cells were harvested and processed for western blotting and IF/FISH co-analyses for Staufen1 and vRNA. gp120 (Env) was stably expressed but Gag and Gag-Pol were not, as expected (Fig. 7A). Some 26% of cellular Staufen1 colocalized with vRNA (Table 1). In cells in which Staufen1 was depleted, we noted again larger Staufen1 punctae in pNL4-XX-expressing cells and a doubling of the extent to which Staufen1 colocalized with vRNA (to 60±10%, mean ± s.d.), consistent with a lowered abundance of cellular Staufen1 and little increase in the total amount of Staufen1 colocalizing with vRNA (Table 1). This also indicated that the association of Staufen1 to vRNA was probably not significantly affected when it was in limiting supply. We did not detect any significant plasma membrane localization when Staufen1 was depleted in cells (Fig. 7B), indicating that Gag expression might be involved in the localization of SHRNPs. This would be consistent with our recent findings showing a dependence of Gag on HIV-1 RNP localization (Lehmann et al., 2009).

We then determined whether Gag could be included in the Staufen1-vRNA RNP if Gag expression was rescued in *trans*. In this case, Rev is synthesized from pNL4-XX and a *gag* RNA is derived from a Rev-dependent Gag expressor supplied in *trans* (Lingappa et al., 2006). Gag was only expressed when pNL4-XX was coexpressed and, in si55/63 conditions, the decrease in Gag synthesis was again observed (Fig. 7A). Confocal imaging analyses for Staufen1, vRNA and Gag revealed that whereas the

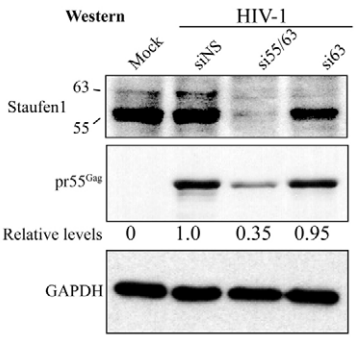

Fig. 6. Staufen1 depletion downregulates Gag expression. HeLa cells were transfected as described in Fig. 1. Numbers below $pr55^{Gag}$ (Gag) western blotting lanes correspond to relative levels of Gag compared to siNS condition (calculated for this experiment).

colocalization between Staufen1 and vRNA was maintained, Gag was not recruited to Staufen1-vRNA RNPs when it was expressed in *trans* (Fig. 7C). Furthermore, the larger RNPs that were found to be devoid of Gag had low immune reactivity for PABP1 (Fig. 7C), and this was found in the majority of cells (70%) in three experiments. Therefore, in order for a SHRNP to form that contains Gag, there might be a requirement for *cis* translation of the *gag* mRNA (i.e. vRNA) and the co-translational recruitment of Gag to Staufen1-vRNA complexes. This could also prevent the formation of typical SG in HIV-1-expressing cells by excluding PABP1. This result also supports the notion that SHRNP formation requires ongoing translation.

Staufen1 depletion enhances vRNA encapsidation

Finally, we studied the consequences of Staufen1 depletion and the remodelling of SHRNPs on the HIV-1 replication cycle. Because Staufen1 is a virion-associated protein (Mouland et al., 2000; Kozak et al., 2006), we determined whether there were any compositional differences between purified HIV-1 derived from control (siNS) and Staufen1-depleted cells. Cells were harvested for western blot and RT-PCR analyses. Virus was purified from cell supernatants and quantified by a sensitive ELISA that detects the mature Gag product, p24; this result was routinely confirmed by western blotting analyses for virion-associated Gag (Fig. 9B and data not shown). vRNA was isolated from cells, and equal quantities of virus were quantified by semi-quantitative RT-PCR. Whereas cellular levels of vRNA remained relatively unchanged, si55/63 enhanced the abundance of vRNA in virus particles (Fig. 8A). This enrichment of virion-associated vRNA was reproducible in different settings, using different proviral strains and siRNA targets and being measured by different methods (data not shown). Indeed, using shRNA to deplete intracellular Staufen1 (Fig. 1C), we confirmed that vRNA encapsidation was enhanced over twofold during the expression of an isogenic protease-negative provirus (HxBRU Pr–; Fig. 8B; corresponding expression blots are shown in Fig. 9B). The increases in vRNA encapsidation in both si55/63 and shSTF conditions ranged from 1.7- to 4.5-fold (3.6±0.5-fold, mean ± s.e.m., eight experiments). Thus, the depletion of Staufen1 from HIV-1-expressing cells consistently results in enhanced vRNA encapsidation.

Because vRNA encapsidation might be coupled to dimerization (Ooms et al., 2004), we then tested whether Staufen1 influences vRNA dimerization. Despite an efficient knockdown of Staufen1

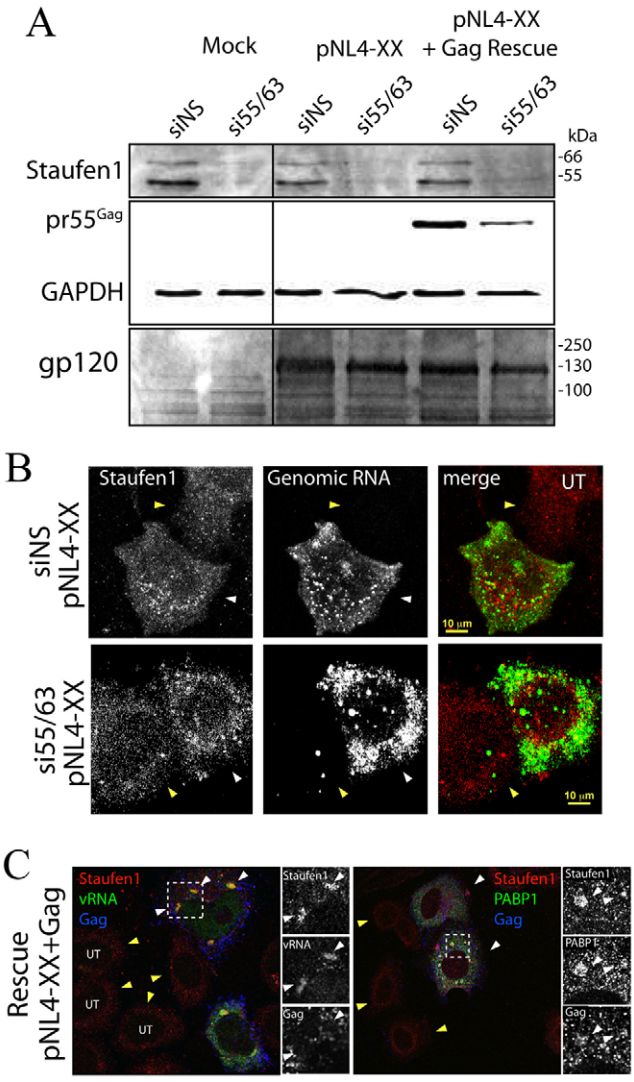

Fig. 7. Staufen1-vRNA RNPs form in the absence of Gag expression. HeLa cells were mock-transfected or transfected with proviral DNA (pNL4-XX, harbouring two mutations to prevent Gag synthesis) and siNS or si55/63 and were harvested and fixed 36-40 hours later for western blotting and IF/FISH analyses. (**A**) Western blotting for Staufen1, GAPDH (loading control) and gp120 (Env). (**B**) Cells were stained for Staufen1 (red) and vRNA (green) in siNS and si55/63 conditions expressing pNL4-XX. (**C**) Gag expression was rescued with GagRRE when expressed in *trans* with pNL4-XX and cells were stained for Staufen1 (red), vRNA (green) and Gag (blue; left panel) or for Staufen1 (red), PABP1 (green) and Gag (blue; right panel). HIV-1-expressing cells are indicated by white arrowheads and HIV-1-negative cells are identified by yellow arrowheads. UT, untransfected cell. Scale bars: 10 µm.

expression by 90% (the corresponding western blots for this experiment are shown in Fig. 6), the melting curves for vRNA dimers derived from siRNA-treated cells were found to be similar (Fig. 8C), ruling out an influence of Staufen1 on vRNA dimerization and stability.

To examine the protein content of virus in these conditions, we performed western blotting on extracts from cells and purified virus. Equal protein quantities (for cell extracts) and equal p24-equivalents of virus were loaded onto SDS-PAGE gels. $Staufen1^{55kDa}$ was efficiently depleted by 90% in si55/63-treated cells when compared

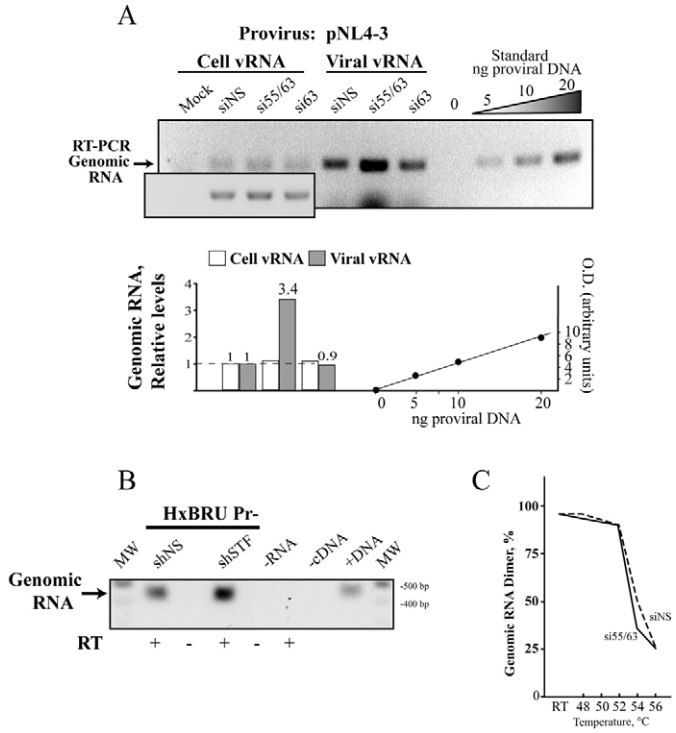

Fig. 8. Virological determinations in cells treated with siNS, si55/63 or si63. (**A**) Cellular and viral RNA were analysed by RT-PCR. HxBRU DNA was used to generate a standard curve. Numbers above histograms represent the fold induction over siNS treatment control from the experiment shown. The inset shows PCR product for cell-associated vRNA levels following ten additional PCR cycles. (**B**) RT-PCR analysis for virus derived from cells expressing HxBRU Pr–. Negative controls included the exclusion of RNA (–RNA) in the RT reaction and the exclusion of cDNA products (–cDNA) in the PCR reaction. 1 ng proviral DNA (+DNA) served as a positive control for the PCR. (**C**) Dimerization analysis of vRNA isolated from virus from siNS (dashed line) and si55/63-treated (solid line) cells.

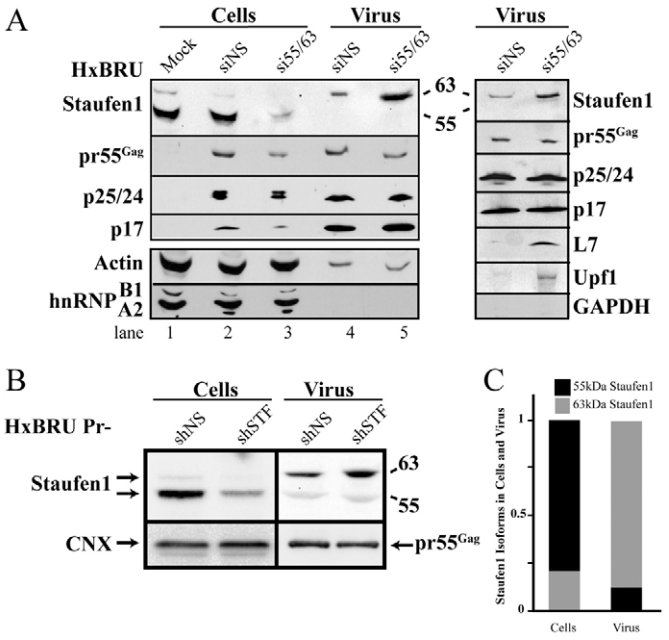

Fig. 9. Cellular and viral protein expression levels following either siNS or si55/63 treatment. (**A**) Cells were mock-transfected (lane 1) or co-transfected with the HxBRU proviral DNA and either siNS (lanes 2 and 4) or si55/63 (lanes 3 and 5). Cell extracts and purified virus were prepared. Cell extracts (lanes 1-3) and corresponding virus (lanes 4,5) were subjected to western analyses for Staufen1, MAp17, actin and hnRNPA2/B1. Equivalent loading of viral extracts is shown by similar signal intensities of Gag proteins in the viral samples (lanes 4,5). Right: an independent experiment was performed exactly as described in A. Western blotting was performed for Staufen1 and Gag proteins, MAp17, ribosomal protein L7, GAPDH and Upf1. (**B**) Western blotting for Staufen1 and Calnexin (CNX, loading control) and Staufen1 and $pr55^{Gag}$ in viral extracts from cells expressing HxBRU Pr–. (**C**) The stacked histogram reveals the reversal in the relative abundance of the two Staufen1 isoforms in cell and viral extracts (averages from five experiments).

to mock- or siNS-treated cells. Cellular Gag levels were diminished to a similar extent in si55/63 conditions (Fig. 9A). si55/63 treatment led to a several-fold increase in the abundance of virus-associated $Staufen1^{63kDa}$ as shown in western blots for Staufen1 (Fig. 9A). Actin levels in the viruses were constant regardless of treatment. The presence and absence of actin and heterogeneous nuclear (hn)RNP A2/B1 in purified virus served as positive and negative virion-associated protein controls, respectively (Liu et al., 1999; Mouland et al., 2001). In an independent experiment, the abundance of ribosomal L7 and the major nonsense-mediated decay protein, Upf1, two proteins that have been identified in Staufen1 complexes (Brendel et al., 2004; Kim et al., 2005) and the HIV-1 RNP (Ajamian et al., 2008), were also increased in highly purified virus from Staufen1-depleted cells (Fig. 9A, right panel). These results show that Staufen1 depletion induces a selective salvaging of the $Staufen1^{63kDa}$ isoform in virus.

We also depleted Staufen1 by shSTF during the expression of a protease-negative provirus. In this experiment, Staufen1 expression was depleted by 85% (Fig. 9B). The depletion of both Staufen1 isoforms again promoted the preferential encapsidation of $Staufen1^{63kDa}$ in virus (1.9-fold increase; Fig. 9B). Western blot analyses for virion-associated Gag ($pr55^{Gag}$) demonstrated equal loading of virus. Levels of $Staufen1^{55kDa}$ detected in viral lysates did not markedly change and the relative abundance of the two Staufen1 isoforms in cells and virus was reversed. This result indicates that $Staufen1^{63kDa}$ is available for encapsidation and that when Staufen1 expression is compromised, it is salvaged, like the vRNA, into de novo synthesized virus particles, probably via the formation of SHRNPs in these conditions.

Discussion

In mammalian cells, Staufen proteins are found in RNPs of molecular weight 440-670 kDa that are thought to represent RNA trafficking granules and to be involved in the repositioning and translational activity of polysome-bound mRNAs (Brendel et al., 2004; Kohrmann et al., 1999; Mallardo et al., 2003). Our earlier observations that indicated a relationship between Staufen1 and the selection of vRNA by Gag are followed up in this study in which we now provide evidence for a role for Staufen1 in vRNA encapsidation. First, we demonstrate that HIV-1 recruits Staufen1 to form distinct, intracellular HIV-1-dependent SHRNPs and that these appear as larger foci in intracellular domains when Staufen1 is in limiting supply. Second, the striking correlation between the formation of larger, visible SHRNP foci and an increased abundance of vRNA in virions suggests that SHRNPs might represent vRNA-containing scaffolds through which vRNA is trafficked and

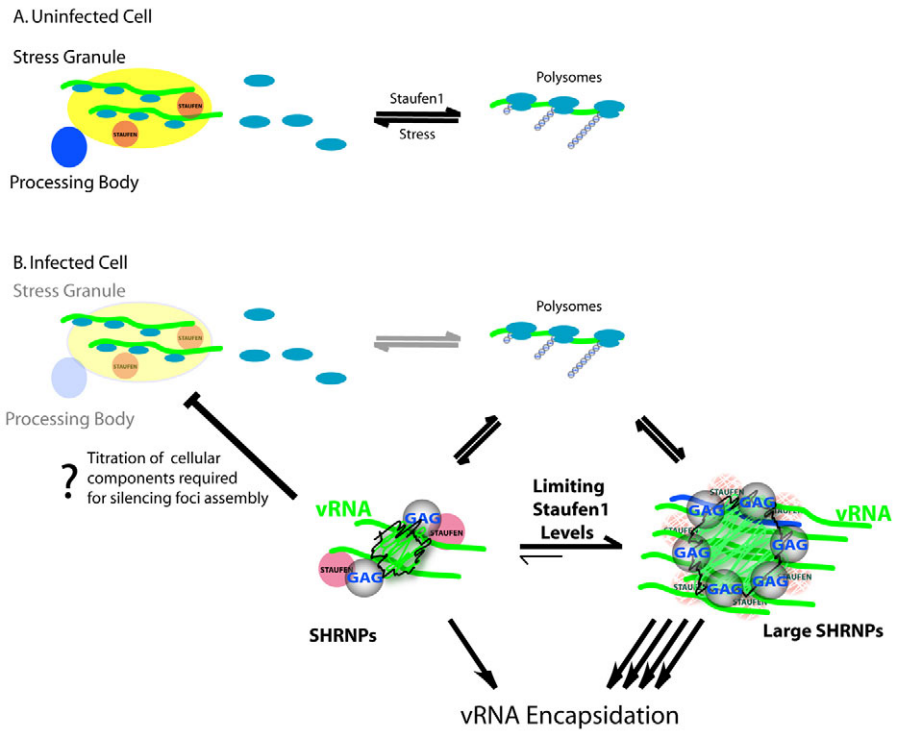

Fig. 10. HIV-1 affects cellular silencing foci and promotes the formation of specific RNA granules. (**A**) PBs and SGs are present in non-infected cells. Silencing foci size and number depends on stress levels, and both PBs and SGs are in dynamic equilibrium with polysomes. The double-stranded RNA-binding protein Staufen1 downregulates SG formation. (**B**) After HIV-1 infection, PBs and stress-induced SGs do not form and specific particles containing vRNA, Gag and cellular Staufen1 (termed SHRNPs) form leading to the encapsidation of vRNA. Gag is dispensable for their formation. SHRNP assembly is in equilibrium with translating polysomes and resembles the behaviour of cellular silencing foci in A. Staufen1 depletion enhances the apparent size of SHRNP foci in cells representing either coalesced SHRNPs or enlarged SHRNPs (shown) to facilitate vRNA encapsidation.

encapsidated into assembling HIV-1. Staufen1-containing RNPs form with or without the presence of Gag and are bona fide RNPs rather than preformed viral particles.

The colocalization of Staufen1 with vRNA and Gag, and the increase in the apparent size of SHRNPs that correlated with vRNA encapsidation levels (Figs 1 and 8), both suggest that Staufen1 is a relevant host factor during the selection of HIV-1 vRNA during assembly. The observed changes in size and content of SHRNPs are probably due to the accumulation of vRNA, whose fate and trafficking depend on Staufen1. A notable analogy can be drawn: in cases in which decapping enzymes have been depleted, small and poorly visible PBs become supraphysiologic in size and accumulate RNA substrates (Franks and Lykke-Andersen, 2007). Whether the increased size of SHRNPs in Staufen1-depleted cells represents an increase in size of the Staufen1 RNP or represents the coalescing of multiple SHRNPs remains to be determined. However, when we observe SHRNPs, HIV-1 expression alone can induce compositional changes to Staufen1 RNPs in cells (Ajamian et al., 2008), and modulation of Staufen1 levels enhances insoluble Gag complexes (Chatel-Chaix et al., 2007). SHRNP localization was also found to be partly coincident with the perinuclear region where vRNA and Gag have been shown to physically interact (Poole et al., 2005) and to which targeting of vRNA has been shown to lead to enhanced vRNA encapsidation (Levesque et al., 2006). From a mechanistic standpoint, the formation of larger RNPs could explain the deregulation of assembly and enhanced encapsidation of vRNA, Staufen1^{63kDa} and other Staufen1-binding proteins found in the HIV-1 RNP such as Upf1 (Ajamian et al., 2008). In addition, it could explain the deleterious effects we have demonstrated on infectivity (Chatel-Chaix et al., 2004). This is not without precedence. For example, Resh and colleagues showed that Gag transits through intracellular bodies before being trafficked to the plasma membrane (Martinez et al., 2008), and the selective knockdown of cellular RNA-binding proteins blocks HIV-1 RNA transport at distinct intracellular loci (Levesque et al., 2006). This type of selectivity of a Staufen RNP was also found in *Drosophila* in the Sponge-Body (Snee and Macdonald, 2009). Moreover, the 'T-body' RNP harbours the Ty1 retrotransposon genomic RNA and a Gag-like protein and was suggested to serve as a scaffold for viral RNA trafficking and assembly (Malagon and Jensen, 2008). Furthermore, large intracellular RNPs form during flavivirus replication and these contribute to genomic RNA encapsidation (Emara and Brinton, 2007). Other RNPs that contain Staufen are relevant for RNA trafficking and for virus restriction (Chiu et al., 2006; Gallois-Montbrun et al., 2007; Kozak et al., 2006; Menager et al., 2009). The SHRNP probably represents an RNP that is specifically engineered by HIV-1 to constitute an intermediary compartment to which vRNA is trafficked for selection by Gag. Further study of the SHRNP will be important in order to understand in what context it is found in cells and to develop a more complete understanding of the fate of the genomic RNA during HIV-1 assembly.

Virus infection can induce a cellular stress response and the formation of SGs (Gale et al., 2000; McInerney et al., 2005) but, conversely, several viruses have developed mechanisms to counteract cellular stress responses that can impose severe limitations to viral replication. Although both SG and SHRNP assembly depend on active translation, the SHRNPs that we have identified after Staufen1 depletion as well as in cells with normal levels of Staufen1 are distinct from the known Staufen1-containing SGs identified in earlier work (Thomas et al., 2005) (supplementary material Fig. S2). Pur, however, leads to the remodelling of SHRNPs by displacing Gag from Staufen1-vRNA-containing RNPs, thus demonstrating that SHRNPs are plastic in nature as are other Staufen-containing RNPs (Snee and Macdonald, 2009). Knockdown of Staufen1 enhances SG formation in murine cells but SGs in this particular case are devoid of Staufen1, leading to the notion that this host protein monitors stress responses in cells without being crucial to SG assembly (Thomas et al., 2009). This result perhaps

parallels what is actually occurring in HIV-1-expressing cells in which the assembly of SHRNPs is favoured over that of SG. The Staufen1-, vRNA- and Gag-containing SHRNPs did not contain PABP1, indicating the preference towards SHRNP formation even when oxidative stress was induced by Ars in HIV-1-producing cells (Figs 4, 5 and supplementary material Fig. S1). Consistently, HIV-1 protease cleaves PABP1 and this could provide further substantive evidence that HIV-1 needs to deactivate PABP1 function (Alvarez et al., 2006) to favour the assembly of SHRNPs during the late stages of replication.

How and why HIV-1 dramatically impairs the assembly of Ars-induced SGs (Fig. 4, 5 and supplementary material Fig. S1) but not that of Pur-induced SGs remain important questions. Ars and Pur elicit the formation of SG by distinct mechanisms. For example, Pur induces SG by disassembling polysomes whereas Ars induces SGs by eliciting eIF2α phosphorylation to result in a block to the recycling of the translation ternary complex (Farny et al., 2009; Kedersha et al., 2000). Because HIV-1 expression did not promote the phosphorylation of eIF2α in basal conditions, nor did it impair Ars-induced eIF2α phosphorylation (Fig. 4), the inhibition of SGs is probably not due to a block to eIF2α phosphorylation as reported for other viruses (Gale et al., 2000; Schneider and Mohr, 2003). Future work will help unravel how HIV-1 blocks SG assembly and whether other retroviruses have the same effect. The phenotype we observed in this study is similar to a stress-resistant phenotype characterized for Semliki Forest Virus (McInerney et al., 2005). Likewise, HIV-1 has evolved strategies to prevent a stress response that might lead to apoptosis and cell death (Dayton, 2008). We propose that SG formation is blocked by HIV-1 to prevent deleterious effects on viral replication and this might be achieved by preventing the recruitment of key components required for SG assembly.

Given that polysomes, SGs and PBs are believed to be in a dynamic equilibrium (Eulalio et al., 2007; Kedersha et al., 2000) and share several components [Staufen1 for instance (Kedersha et al., 2005)], we examined the relationship between SHRNPs and PBs, the latter representing cytoplasmic RNPs involved in mRNA metabolism and storage (Bruno and Wilkinson, 2006). Although it was only our intent to rule out that SHRNPs were not PBs, in this manuscript we are able to report two novel and salient findings. First, vRNA, Gag and even Staufen1 were not detectable in PB foci (Fig. 5; and data not shown) and, second, a dramatic decrease in the abundance of PBs was observed in HIV-1-expressing cells and often, PBs were not detectable (Fig. 5). The decrease in size and abundance of PBs has also been noted when expression levels of other cellular proteins are modified or when the translational apparatus is stabilized (Eulalio et al., 2007). Likewise, Staufen1-containing APOBEC3G complexes that could restrict HIV-1 do not cofractionate with PB components (Chiu et al., 2006), and intimations from recent work suggest that PBs might be deleterious to HIV-1 replication (Nathans et al., 2009). We speculate that HIV-1 expression suppresses PB formation or promotes their disassembly by sequestration and/or relocalization of cellular proteins involved in Ars-induced SG and PB assembly or integrity. Recent findings support this idea in that a correlation between the expression of heat-shock protein 72 and SG and PB assembly was drawn (Mazroui et al., 2007). Interesting parallels can also be drawn between our results and those of others in which SGs and PBs cannot form in flavivirus-infected cells due in part to interaction between viral and SG components (Emara and Brinton, 2007). HIV-1 has probably evolved strategies to protect the vRNA from translational silencing and/or degradation in PBs to allow for Gag expression and vRNA selection for encapsidation. HIV-1 inhibits siRNA and miRNA silencing pathways (Bennasser et al., 2005; Triboulet et al., 2007) that actually prevent PB formation (Eulalio et al., 2007), supporting our observation that HIV-1 co-opts RNA degradation machineries to favour viral expression (Ajamian et al., 2008).

The RNA trafficking function of Staufen1 relies on its association with a dimeric RNA in the context of an RNP in *Drosophila* (Ferrandon et al., 1997), although we could not find a link between vRNA dimerization and encapsidation levels (Fig. 8). Because dimerization and encapsidation are coupled processes in HIV-1 (Paillart et al., 2004), it is possible that Staufen1 influences encapsidation via its association to dimeric vRNA. Indeed, MLV genomic RNA selection is influenced by the capacity of Gag to bind vRNA (D'Souza and Summers, 2004). In line with this notion is a recent report that shows that the anti-viral effect of APOBEC3G is controlled by its capacity to bind viral RNA (Soros et al., 2007).

The depletion of Staufen1 led to a decrease in cellular Gag gene expression but this was not due to changes in steady-state vRNA levels (Fig. 8) or Gag protein stability (data not shown). Staufen1 might therefore act as a molecular switch to arrest translation and to favour vRNA encapsidation, a proposed role for EF1α described in an earlier study (Cimarelli and Luban, 1999). An effect on vRNA translation might rely on the ability of Staufen1 to associate to vRNA, because we show that in the presence and absence of Gag and during stress conditions, Staufen1 remains associated with vRNA (Figs 1-4, 7; and data not shown). Alternatively, the close association of Staufen1 to Gag could play a role (Chatel-Chaix et al., 2004). Support for this idea is found in work that shows that Gag levels control the equilibrium between vRNA translation and encapsidation via translational inhibition of vRNA for HIV-1 (Anderson and Lever, 2006) and for the *Idefx* retrotransposon (Meignin et al., 2003). The dynamic link that has been established between translationally silent PBs and Staufen1 RNPs (like that between PBs and SG) (Zeitelhofer et al., 2008) supports the implication of Staufen1 RNPs in translational derepression. The formation of an HIV-1-specific RNP harbouring the components important for vRNA translation and encapsidation is an attractive idea. It will be interesting to determine the compositional differences between these RNPs and the efficiency with which vRNA is translated in SHRNPs.

To our knowledge, few studies have attempted to differentiate between the functions of the Staufen1 isoforms, although evidence indicates that they might be isoform-specific (Duchaine et al., 2000; Duchaine et al., 2002; Macchi et al., 2004). The selective depletion of the larger Staufen1^{63kDa} had little effect on Gag expression levels, on the formation of large SHRNPs or on vRNA encapsidation levels (Figs 1, 8; and data not shown). This isoform is generally less abundant than Staufen1^{55kDa} and a more-subtle phenotype might not be detected using our methods. Conversely, our siRNA and shRNA experiments also show that Staufen1^{63kDa} is preferentially recruited into HIV-1 particles when Staufen1 is depleted in cells. In light of the reproducibility of these results using several knockdown strategies, future work will be needed to understand how and why Staufen1^{63kDa} is preferentially salvaged into virions and the functional relationships that exist between the various protein isoforms.

This work leads to a model in which distinct RNPs form that contain vRNA, Gag, Staufen1 and, probably, other cellular proteins. However, very much like cellular silencing foci (Fig. 10A), in HIV-1 expressing cells these so-called SHRNPs are also in equilibrium

with translating polysomes, because both CHX and Pur affect their assembly. As is the case for SGs, apparent SHRNP size is enhanced by limiting Staufen1 levels (Fig. 10B), probably by mechanisms that involve the stabilization of polysomes. Although SHRNPs could be considered as HIV-1-specific silencing foci, their formation would serve as a scaffold for efficient packaging of the two vRNA molecules selected per virus particle. The inhibition of cellular silencing foci including SGs and PBs is consistent with the ability of HIV-1 to titrate key cellular components in order to assemble functional, virus-specific SHRNPs.

Materials and Methods

Cell culture, proviral, siRNA and shRNA transfections

Transfection of HEK293T and HeLa cells and details on the proviral constructs (HxBRU, pNL4-XX) and siNS and siRNA sequences were described previously (Ajamian et al., 2008; Chatel-Chaix et al., 2004; Mouland et al., 2000). siRNA duplexes and shRNAs were used to knockdown Staufen1 gene expression. The *Staufen1* RNA is alternatively spliced to generate four transcripts. Transcript variant 3 (T3) is the longest and encodes the Staufen1^{63kDa} that contains an additional 81 amino acids in the N-terminus. The transcripts T1, T2 and T4 encode Staufen1^{55kDa} (Fig. 1C). si55/63 (Chatel-Chaix et al., 2004) and si63 (5′-TGAATGGGTCT-ACCTGCATTT-3′) were synthesized (Qiagen-Xeragon) and used at 10 nM. We also performed parallel experiments using additional siRNAs targeted against different regions of *Staufen1* mRNA, and an alternative strategy to knockdown Staufen1 by shRNA. Silencing and non-silencing shRNA (shSTF and shNS) were expressed from an RNA polymerase-II-driven DNA expression vector, as described (Chatel-Chaix et al., 2007). The similarity of results with the multiple siRNAs utilized increases the likelihood that the observed phenotypes were the result of Staufen1 knockdown and not due to off-target effects (Scacheri et al., 2004). Gag expression was rescued in some experiments using a Rev-dependent Gag expressor (from Jaisri Lingappa, University of Washington, Seattle, WA) (Lingappa et al., 2006). Pur and CHX (Sigma-Aldrich) were used at 0.25 mg/ml for 4 hours before fixation. HeLa cells were incubated for 30 minutes with Ars (0.5 mM) at 37°C, washed and incubated for additional 30 minutes at 37°C in fresh medium and then fixed.

Western blotting

At 12-48 hours post-transfection, cells were lysed and equal amounts of protein from cleared post-nuclear supernatant (40 or 50 μg protein) were subjected to SDS-PAGE and western blotting as described (Chatel-Chaix et al., 2004).

IF, FISH and LSCM

IF and combined two-colour IF/FISH analyses were performed as described (Beriault et al., 2004; Levesque et al., 2006). LSCM and image analysis were performed using a Zeiss Pascal LSM5. LSM Image Browser software (Carl Zeiss, Germany) was used to estimate the size of SHRNPs. At least 50 SHRNPs were measured for each condition in at least three experiments. vRNA-containing RNPs that were bigger than 2 μm were excluded from the statistical analysis. PB numbers were calculated by counting DCP-1-positive foci in at least 50 cells from the 10-15 optical fields for each experimental condition. 6× magnifications (Fig. 7) were acquired by LSCM. For other images, higher pixel resolution images to reproduce more detail and subtle colour transitions were obtained by increasing the number of pixels for selected regions in Adobe Photoshop (Adobe). For combined IF/FISH analyses our initial protocol was modified as described (Lehmann et al., 2009): after FISH with a digoxigenin-labelled probe, vRNA was visualized by staining with biotinylated anti-digoxigenin (Sigma-Aldrich), following by anti-biotin monoclonal antibody conjugated with Alexa Fluor 488 (Invitrogen). The vRNA was visualized in a colour of choice (green or red) due to the Alexa Fluor moiety on this secondary antibody. LSCM was performed at 1024×1024 pixel resolution using the same equipment and settings. Colocalization analyses were performed using Manders' coefficient as described (Ajamian et al., 2008) from at least 15 cells per experimental condition in three experiments. Intensity plots were generated by Imaris software (Bitplane) in the measurement pane through the centre focal plane, as described elsewhere (Lehmann et al., 2009).

Antibodies

A rabbit anti-Staufen1 RLS1 antibody, that recognizes both Staufen1 isoforms was used in IF and western analyses (Thomas et al., 2005). This does not react against Staufen2 in immunofluorescence or western blot analyses. Antibodies to Gag (CA/p24, pr55^{Gag}), MA/p17 polyclonal sheep serum (NIH AIDS Reference and Reagent Program from Michael Phelan), GAPDH, hnRNP A2/B1, anti-tubulin and calnexin are described elsewhere (Beriault et al., 2004; Chatel-Chaix et al., 2004; Levesque et al., 2006; Mouland et al., 2000). Anti-Upf1 and anti-DCP1 were provided by Jens Lykke-Anderson (University of Colorado, Boulder, CO). Anti-PABP1 was provided by Nahum Sonenberg (McGill University, Montreal, Canada), anti-HuR and anti-Ras-GAP SH3 domain binding protein (G3BP) were provided by Imed Gallouzi (McGill University, Montreal, Canada) and anti eIF3η was purchased from Santa Cruz Biotechnology. Anti-actin, anti-eIF2α-*P*, anti-pan-eIF2α were purchased from Abcam; anti-L7, anti-EF1α, anti-PABP1 and anti-GAPDH were purchased from Novus Biologicals, Upstate, Sigma-Aldrich and TechniScience, respectively. A goat anti-gp120 (Env) was obtained from the NIH (#385, from Kathelyn Steimer). The secondary antibodies were anti-rabbit-Alexa-Fluor-594, anti-mouse-Alexa-Fluor-488, -594 or -647 and anti-sheep-Alexa-Fluor-647 (Invitrogen).

vRNA dimerization analyses

Dimerization analysis was performed using RNA extracted from 5 μg p24-equivalents virus as described (Laughrea and Jette, 1997).

RT-PCR of Staufen1 and HIV-1 RNAs

Total RNA or viral RNA was extracted by Trizol reagent and subjected to SuperScript One-Step RT-PCR (Beriault et al., 2004; Chatel-Chaix et al., 2004). Virus was quantified by p24-ELISA and equal amounts of virus were used in subsequent RNA extraction. RNA was treated with DNAse I, repurified and used in RT-PCR. Staufen1 primers were designed to amplify portions of the T3 and T2 transcripts to generate 540 bp and 270 bp PCR products, respectively: sense primer (nt 140-169) and antisense primer (nt 670-699) of the *Staufen1* cDNA (NM017453). *gapdh* RNA was quantified by RT-PCR as described (Levesque et al., 2006).

Sequential affinity-based immunoprecipitation and RT-PCR

HeLa cells were mock-transfected with FLAG epitope-tagged Staufen1 expressor (Staufen1-FLAG; (Chatel-Chaix et al., 2008) or transfected with proviral DNA (pNL4-3) and Staufen1-FLAG. At 30-36 hours post-transfection, total cell lysates were collected in a Nonidet P40 lysis buffer (Chatel-Chaix et al., 2007). An aliquot representing 3% of the cell lysate (input) was used for western blotting for Staufen1-FLAG, Gag and GAPDH. 1 mg protein was immunoprecipitated with FLAG-agarose beads (Sigma-Aldrich) and then eluted with excess FLAG peptide (Sigma-Aldrich) according to the manufacturer's instructions. 10% of this eluate was assessed by western blotting to measure the recovery of Staufen1-FLAG and then Gag was immunoprecipitated from the first eluate with affinity-purified mouse anti-p24 monoclonal antibody (Ajamian et al., 2008). The immune complex was then eluted by 0.1 M glycine-HCl (pH 2.5). The RNA was purified using Trizol LS (Invitrogen). 10% of each immunoprecipitate was collected for western blotting analysis. 1 μg of input total cellular RNA and 50% of that isolated from the immunoprecipitate were used for RT-PCR. RT-PCR was performed for vRNA and *gapdh* mRNA as described above.

We thank Imed Gallouzi for critical reading of the manuscript and helpful discussions and Jens Lykke-Andersen, Nahum Sonenberg, Imed Gallouzi, William Rigby, Koren Mann, David Ott, Jaisri Lingappa, Kathelyn Steimer, Michael Phelan and the NIH AIDS Reference and Reagent Program for reagents and antibodies. Anne Monette and Lara Ajamian are recipients of Canadian Institutes of Health Research (CIHR) Doctoral fellowships and A.J.M. was supported by a CIHR New Investigator and FRSQ Chercheur-boursier Senior career awards. This work was supported by grants from the Canadian Foundation for Innovation and the CIHR (MOP-38111, MOP-56794, OPC-83178) to A.J.M.

Supplementary material available online at
http://jcs.biologists.org/cgi/content/full/123/3/369/DC1

References

Ajamian, L., Abrahamyan, L., Milev, M., Ivanov, P. V., Kulozik, A. E., Gehring, N. H. and Mouland, A. J. (2008). Unexpected roles for UPF1 in HIV-1 RNA metabolism and translation. *RNA* **14**, 914-927.

Alvarez, E., Castello, A., Menendez-Arias, L. and Carrasco, L. (2006). HIV protease cleaves poly(A)-binding protein. *Biochem. J.* **396**, 219-226.

Anderson, E. C. and Lever, A. M. (2006). Human immunodeficiency virus type 1 Gag polyprotein modulates its own translation. *J. Virol.* **80**, 10478-10486.

Anderson, P. and Kedersha, N. (2008). Stress granules: the Tao of RNA triage. *Trends Biochem. Sci.* **33**, 141-150.

Barbee, S. A., Estes, P. S., Cziko, A. M., Hillebrand, J., Luedeman, R. A., Coller, J. M., Johnson, N., Howlett, I. C., Geng, C., Ueda, R. et al. (2006). Staufen- and FMRP-containing neuronal RNPs are structurally and functionally related to somatic P bodies. *Neuron* **52**, 997-1009.

Beckham, C. J. and Parker, R. (2008). P bodies, stress granules, and viral life cycles. *Cell Host Microbe* **3**, 206-212.

Beliakova-Bethell, N., Beckham, C., Giddings, T. H., Jr, Winey, M., Parker, R. and Sandmeyer, S. (2006). Virus-like particles of the Ty3 retrotransposon assemble in association with P-body components. *RNA* **12**, 94-101.

Bennasser, Y., Le, S. Y., Benkirane, M. and Jeang, K. T. (2005). Evidence that HIV-1 encodes an siRNA and a suppressor of RNA silencing. *Immunity* **22**, 607-619.

Beriault, V., Clement, J. F., Levesque, K., Lebel, C., Yong, X., Chabot, B., Cohen, E. A., Cochrane, A. W., Rigby, W. F. and Mouland, A. J. (2004). A late role for the association of hnRNP A2 with the HIV-1 hnRNP A2 response elements in genomic RNA, Gag, and Vpr localization. *J. Biol. Chem.* **279**, 44141-44153.

Brendel, C., Rehbein, M., Kreienkamp, H. J., Buck, F., Richter, D. and Kindler, S. (2004). Characterization of Staufen 1 ribonucleoprotein complexes. *Biochem. J.* **384**, 239-246.

Bruno, I. and Wilkinson, M. F. (2006). P-bodies react to stress and nonsense. *Cell* **125**, 1036-1038.

Butsch, M. and Boris-Lawrie, K. (2000). Translation is not required To generate virion precursor RNA in human immunodeficiency virus type 1-infected T cells. *J. Virol.* **74**, 11531-11537.

Chatel-Chaix, L., Clement, J. F., Martel, C., Beriault, V., Gatignol, A., DesGroseillers, L. and Mouland, A. J. (2004). Identification of Staufen in the human immunodeficiency virus type 1 Gag ribonucleoprotein complex and a role in generating infectious viral particles. *Mol. Cell. Biol.* **24**, 2637-2648.

Chatel-Chaix, L., Abrahamyan, L., Frechina, C., Mouland, A. J. and DesGroseillers, L. (2007). The host protein Staufen1 participates in human immunodeficiency virus type 1 assembly in live cells by influencing pr55Gag multimerization. *J. Virol.* **81**, 6216-6230.

Chatel-Chaix, L., Boulay, K., Mouland, A. J. and Desgroseillers, L. (2008). The host protein Staufen1 interacts with the Pr55Gag zinc fingers and regulates HIV-1 assembly via its N-terminus. *Retrovirology* **5**, 41.

Chiu, Y. L., Witkowska, H. E., Hall, S. C., Santiago, M., Soros, V. B., Esnault, C., Heidmann, T. and Greene, W. C. (2006). High-molecular-mass APOBEC3G complexes restrict Alu retrotransposition. *Proc. Natl. Acad. Sci. USA* **103**, 15588-15593.

Cimarelli, A. and Luban, J. (1999). Translation elongation factor 1-alpha interacts specifically with the human immunodeficiency virus type 1 Gag polyprotein. *J. Virol.* **73**, 5388-5401.

Dahm, R., Zeitelhofer, M., Gotze, B., Kiebler, M. A. and Macchi, P. (2008). Visualizing mRNA localization and local protein translation in neurons. *Methods Cell Biol.* **85**, 293-327.

Dayton, A. I. (2008). Hitting HIV where it hides. *Retrovirology* **5**, 15.

De Guzman, R. N., Wu, Z. R., Stalling, C. C., Pappalardo, L., Borer, P. N. and Summers, M. F. (1998). Structure of the HIV-1 nucleocapsid protein bound to the SL3 psi-RNA recognition element. *Science* **279**, 384-388.

D'Souza, V. and Summers, M. F. (2004). Structural basis for packaging the dimeric genome of Moloney murine leukaemia virus. *Nature* **431**, 586-590.

D'Souza, V. and Summers, M. F. (2005). How retroviruses select their genomes. *Nat. Rev. Microbiol.* **3**, 643-655.

Duchaine, T., Wang, H. J., Luo, M., Steinberg, S. V., Nabi, I. R. and DesGroseillers, L. (2000). A novel murine Staufen isoform modulates the RNA content of Staufen complexes. *Mol. Cell. Biol.* **20**, 5592-5601.

Duchaine, T. F., Hemraj, I., Furic, L., Deitinghoff, A., Kiebler, M. A. and DesGroseillers, L. (2002). Staufen2 isoforms localize to the somatodendritic domain of neurons and interact with different organelles. *J. Cell Sci.* **115**, 3285-3295.

Dugre-Brisson, S., Elvira, G., Boulay, K., Chatel-Chaix, L., Mouland, A. J. and DesGroseillers, L. (2005). Interaction of Staufen1 with the 5′ end of mRNA facilitates translation of these RNAs. *Nucleic Acids Res.* **33**, 4797-4812.

Emara, M. M. and Brinton, M. A. (2007). Interaction of TIA-1/TIAR with West Nile and dengue virus products in infected cells interferes with stress granule formation and processing body assembly. *Proc. Natl. Acad. Sci. USA* **104**, 9041-9046.

Eulalio, A., Behm-Ansmant, I., Schweizer, D. and Izaurralde, E. (2007). P-body formation is a consequence, not the cause, of RNA-mediated gene silencing. *Mol. Cell. Biol.* **27**, 3970-3981.

Farny, N. G., Kedersha, N. L. and Silver, P. A. (2009). Metazoan stress granule assembly is mediated by P-eIF2alpha-dependent and -independent mechanisms. *RNA* **15**, 1814-1821.

Ferrandon, D., Koch, I., Westhof, E. and Nusslein-Volhard, C. (1997). RNA-RNA interaction is required for the formation of specific bicoid mRNA 3′ UTR-STAUFEN ribonucleoprotein particles. *EMBO J.* **16**, 1751-1758.

Franks, T. M. and Lykke-Andersen, J. (2007). TTP and BRF proteins nucleate processing body formation to silence mRNAs with AU-rich elements. *Genes Dev.* **21**, 719-735.

Gale, M., Jr, Tan, S. L. and Katze, M. G. (2000). Translational control of viral gene expression in eukaryotes. *Microbiol. Mol. Biol. Rev.* **64**, 239-280.

Gallois-Montbrun, S., Kramer, B., Swanson, C. M., Byers, H., Lynham, S., Ward, M. and Malim, M. H. (2007). Antiviral protein APOBEC3G localizes to ribonucleoprotein complexes found in P bodies and stress granules. *J. Virol.* **81**, 2165-2178.

Jonson, L., Vikesaa, J., Krogh, A., Nielsen, L. K., Hansen, T. V., Borup, R., Johnsen, A. H., Christiansen, J. and Nielsen, F. C. (2007). Molecular composition of IMP1 ribonucleoprotein granules. *Mol. Cell Proteomics* **6**, 798-811.

Kaye, J. F. and Lever, A. M. (1999). Human immunodeficiency virus types 1 and 2 differ in the predominant mechanism used for selection of genomic RNA for encapsidation. *J. Virol.* **73**, 3023-3031.

Kedersha, N. L., Gupta, M., Li, W., Miller, I. and Anderson, P. (1999). RNA-binding proteins TIA-1 and TIAR link the phosphorylation of eIF-2 alpha to the assembly of mammalian stress granules. *J. Cell Biol.* **147**, 1431-1442.

Kedersha, N., Cho, M. R., Li, W., Yacono, P. W., Chen, S., Gilks, N., Golan, D. E. and Anderson, P. (2000). Dynamic shuttling of TIA-1 accompanies the recruitment of mRNA to mammalian stress granules. *J. Cell Biol.* **151**, 1257-1268.

Kedersha, N., Chen, S., Gilks, N., Li, W., Miller, I. J., Stahl, J. and Anderson, P. (2002). Evidence that ternary complex (eIF2-GTP-tRNA(i)(Met))-deficient preinitiation complexes are core constituents of mammalian stress granules. *Mol. Biol. Cell* **13**, 195-210.

Kedersha, N., Stoecklin, G., Ayodele, M., Yacono, P., Lykke-Andersen, J., Fritzler, M. J., Scheuner, D., Kaufman, R. J., Golan, D. E. and Anderson, P. (2005). Stress granules and processing bodies are dynamically linked sites of mRNP remodeling. *J. Cell Biol.* **169**, 871-884.

Kim, Y. K., Furic, L., Desgroseillers, L. and Maquat, L. E. (2005). Mammalian Staufen1 recruits Upf1 to specific mRNA 3′UTRs so as to elicit mRNA decay. *Cell* **120**, 195-208.

Kohrmann, M., Luo, M., Kaether, C., DesGroseillers, L., Dotti, C. G. and Kiebler, M. A. (1999). Microtubule-dependent recruitment of Staufen-green fluorescent protein into large RNA-containing granules and subsequent dendritic transport in living hippocampal neurons. *Mol. Biol. Cell* **10**, 2945-2953.

Kozak, S. L., Marin, M., Rose, K. M., Bystrom, C. and Kabat, D. (2006). The anti-HIV-1 editing enzyme APOBEC3G binds HIV-1 RNA and messenger RNAs that shuttle between polysomes and stress granules. *J. Biol. Chem.* **281**, 29105-29119.

Laughrea, M. and Jette, L. (1997). HIV-1 genome dimerization: kissing-loop hairpin dictates whether nucleotides downstream of the 5′ splice junction contribute to loose and tight dimerization of human immunodeficiency virus RNA. *Biochemistry* **36**, 9501-9508.

Lehmann, M., Milev, M. P., Abrahamyan, L., Yao, X. J., Pante, N. and Mouland, A. J. (2009). Intracellular transport of human immunodeficiency virus type 1 genomic RNA and viral production are dependent on Dynein motor function and late endosome positioning. *J. Biol. Chem.* **284**, 14572-14585.

Levesque, K., Halvorsen, M., Abrahamyan, L., Chatel-Chaix, L., Poupon, V., Gordon, H., DesGroseillers, L., Gatignol, A. and Mouland, A. J. (2006). Trafficking of HIV-1 RNA is mediated by heterogeneous nuclear ribonucleoprotein A2 expression and impacts on viral assembly. *Traffic* **7**, 1177-1193.

Lingappa, J. R., Dooher, J. E., Newman, M. A., Kiser, P. K. and Klein, K. C. (2006). Basic residues in the nucleocapsid domain of Gag are required for interaction of HIV-1 gag with ABCE1 (HP68), a cellular protein important for HIV-1 capsid assembly. *J. Biol. Chem.* **281**, 3773-3784.

Liu, B., Dai, R., Tian, C. J., Dawson, L., Gorelick, R. and Yu, X. F. (1999). Interaction of the human immunodeficiency virus type 1 nucleocapsid with actin. *J. Virol.* **73**, 2901-2908.

Macchi, P., Brownawell, A. M., Grunewald, B., DesGroseillers, L., Macara, I. G. and Kiebler, M. A. (2004). The brain-specific double-stranded RNA-binding protein Staufen2: nucleolar accumulation and isoform-specific exportin-5-dependent export. *J. Biol. Chem.* **279**, 31440-31444.

Malagon, F. and Jensen, T. H. (2008). The T body, a new cytoplasmic RNA granule in Saccharomyces cerevisiae. *Mol. Cell. Biol.* **28**, 6022-6032.

Mallardo, M., Deitinghoff, A., Muller, J., Goetze, B., Macchi, P., Peters, C. and Kiebler, M. A. (2003). From the cover: isolation and characterization of Staufen-containing ribonucleoprotein particles from rat brain. *Proc. Natl. Acad. Sci. USA* **100**, 2100-2105.

Martinez, N. W., Xue, X., Berro, R. G., Kreitzer, G. and Resh, M. D. (2008). Kinesin KIF4 regulates intracellular trafficking and stability of the human immunodeficiency virus type 1 Gag polyprotein. *J. Virol.* **82**, 9937-9950.

Mazroui, R., Di Marco, S., Kaufman, R. J. and Gallouzi, I. E. (2007). Inhibition of the ubiquitin-proteasome system induces stress granule formation. *Mol. Biol. Cell.* **18**, 2603-2618.

McInerney, G. M., Kedersha, N. L., Kaufman, R. J., Anderson, P. and Liljestrom, P. (2005). Importance of eIF2alpha phosphorylation and stress granule assembly in alphavirus translation regulation. *Mol. Biol. Cell* **16**, 3753-3763.

Meignin, C., Bailly, J. L., Arnaud, F., Dastugue, B. and Vaury, C. (2003). The 5′ untranslated region and Gag product of Idefix, a long terminal repeat-retrotransposon from Drosophila melanogaster, act together to initiate a switch between translated and untranslated states of the genomic mRNA. *Mol. Cell. Biol.* **23**, 8246-8254.

Menager, P., Roux, P., Megret, F., Bourgeois, J. P., Le Sourd, A. M., Danckaert, A., Lafage, M., Prehaud, C. and Lafon, M. (2009). Toll-like receptor 3 (TLR3) plays a major role in the formation of rabies virus Negri Bodies. *PLoS Pathog.* **5**, e1000315.

Monshausen, M., Gehring, N. H. and Kosik, K. S. (2004). The mammalian RNA-binding protein Staufen2 links nuclear and cytoplasmic RNA processing pathways in neurons. *Neuromolecular Med.* **6**, 127-144.

Mouland, A. J., Mercier, J., Luo, M., Bernier, L., DesGroseillers, L. and Cohen, E. A. (2000). The double-stranded RNA-binding protein Staufen is incorporated in human immunodeficiency virus type 1, evidence for a role in genomic RNA encapsidation. *J. Virol.* **74**, 5441-5451.

Mouland, A. J., Xu, H., Cui, H., Krueger, W., Munro, T. P., Prasol, M., Mercier, J., Rekosh, D., Smith, R., Barbarese, E. et al. (2001). RNA trafficking signals in human immunodeficiency virus type 1. *Mol. Cell. Biol.* **21**, 2133-2143.

Nathans, R., Chu, C. Y., Serquina, A. K., Lu, C. C., Cao, H. and Rana, T. M. (2009). Cellular microRNA and P bodies modulate host-HIV-1 interactions. *Mol. Cell* **34**, 696-709.

Ooms, M., Huthoff, H., Russell, R., Liang, C. and Berkhout, B. (2004). A riboswitch regulates RNA dimerization and packaging in human immunodeficiency virus type 1 virions. *J. Virol.* **78**, 10814-10819.

Paillart, J. C., Shehu-Xhilaga, M., Marquet, R. and Mak, J. (2004). Dimerization of retroviral RNA genomes: an inseparable pair. *Nat. Rev. Microbiol.* **2**, 461-472.

Poole, E., Strappe, P., Mok, H. P., Hicks, R. and Lever, A. M. (2005). HIV-1 Gag-RNA interaction occurs at a perinuclear/centrosomal site; analysis by confocal microscopy and FRET. *Traffic* **6**, 741-755.

Poon, D. T., Chertova, E. N. and Ott, D. E. (2002). Human immunodeficiency virus type 1 preferentially encapsidates genomic RNAs that encode Pr55(Gag): functional linkage between translation and RNA packaging. *Virology* **293**, 368-378.

Scacheri, P. C., Rozenblatt-Rosen, O., Caplen, N. J., Wolfsberg, T. G., Umayam, L., Lee, J. C., Hughes, C. M., Shanmugam, K. S., Bhattacharjee, A., Meyerson, M. et al. (2004). Short interfering RNAs can induce unexpected and divergent changes in the levels of untargeted proteins in mammalian cells. *Proc. Natl. Acad. Sci. USA* **101**, 1892-1897.

Schneider, R. J. and Mohr, I. (2003). Translation initiation and viral tricks. *Trends Biochem. Sci.* **28**, 130-136.

Snee, M. J. and Macdonald, P. M. (2009). Dynamic organization and plasticity of sponge bodies. *Dev. Dyn.* **238**, 918-930.

Soros, V. B., Yonemoto, W. and Greene, W. C. (2007). Newly synthesized APOBEC3G is incorporated into HIV virions, inhibited by HIV RNA, and subsequently activated by RNase H. *PLoS Pathog.* **3**, e15.

St Johnston, D., Beuchle, D. and Nusslein-Volhard, C. (1991). Staufen, a gene required to localize maternal RNAs in the Drosophila egg. *Cell* **66**, 51-63.

Thomas, M. G., Martinez Tosar, L. J., Loschi, M., Pasquini, J. M., Correale, J., Kindler, S. and Boccaccio, G. L. (2005). Staufen recruitment into stress granules does not affect early mRNA transport in oligodendrocytes. *Mol. Biol. Cell* **16**, 405-420.

Thomas, M. G., Tosar, L. J., Desbats, M. A., Leishman, C. C. and Boccaccio, G. L. (2009). Mammalian Staufen 1 is recruited to stress granules and impairs their assembly. *J. Cell Sci.* **122**, 563-573.

Triboulet, R., Mari, B., Lin, Y. L., Chable-Bessia, C., Bennasser, Y., Lebrigand, K., Cardinaud, B., Maurin, T., Barbry, P., Baillat, V. et al. (2007). Suppression of microRNA-silencing pathway by HIV-1 during virus replication. *Science* **315**, 1579-1582.

Vessey, J. P., Macchi, P., Stein, J. M., Mikl, M., Hawker, K. N., Vogelsang, P., Wieczorek, K., Vendra, G., Riefler, J., Tubing, F. et al. (2008). A loss of function allele for murine Staufen1 leads to impairment of dendritic Staufen1-RNP delivery and dendritic spine morphogenesis. *Proc. Natl. Acad. Sci. USA* **105**, 16374-16379.

Villace, P., Marion, R. M. and Ortin, J. (2004). The composition of Staufen-containing RNA granules from human cells indicates their role in the regulated transport and translation of messenger RNAs. *Nucleic Acids Res.* **32**, 2411-2420.

Watts, J. M., Dang, K. K., Gorelick, R. J., Leonard, C. W., Bess, J. W., Jr, Swanstrom, R., Burch, C. L. and Weeks, K. M. (2009). Architecture and secondary structure of an entire HIV-1 RNA genome. *Nature* **460**, 711-716.

Zeitelhofer, M., Karra, D., Macchi, P., Tolino, M., Thomas, S., Schwarz, M., Kiebler, M. and Dahm, R. (2008). Dynamic interaction between P-bodies and transport ribonucleoprotein particles in dendrites of mature hippocampal neurons. *J. Neurosci.* **28**, 7555-7562.